REVIEW

Check for updates

Environmental behavior and human health risks of PFAS: occurrence, toxicity, and the state-of-the-art removal approaches

Pavithra Narasimhappa, [a] Simranjeet Singh, [†a] Radhika Varshney, [a] Vishakha Chauhan, [a] Retinder Kour, [a] Praveen C. Ramamurthy [*a] and Nabila Shehata [b]

Fluorinated compounds, including poly- and per-fluoroalkyl substances (PFAS), are characterized by complex behavior, environmental persistence, and resistance to degradation. These thermally stable compounds repel both oil and water. Concerns are mounting over their bioaccumulation in humans and other organisms, given their associated health risks such as endocrine disruption, immune suppression, obesity, elevated cholesterol levels, and cancer. Low concentrations of PFAS detected in drinking water present a potential human exposure pathway. This review addresses the occurrence and exposure pathways of PFAS; their toxicity in humans, plants, and animals; analytical methods for their detection and quantification in aqueous matrices; and their removal techniques including membrane technologies, advanced oxidation processes, adsorption, ion exchange, biological methods, and hydrothermal liquefaction. The factors affecting the removal of PFAS, such as inorganic anions and cations, natural organic matter, and other organic pollutants in wastewater, are also included. Additionally, cost-effective and environmentally friendly methods for regenerating adsorbents are explored. The conclusion discusses the current restrictions and future perspectives on the analysis of PFAS.

1. Introduction

Poly- and per-fluoroalkyl substances (PFAS) are generated in large quantities and used for industrial processes and consumer products. They belong to organofluorine compounds and are composed of various chains of fluorocarbons and diverse functional groups.[1,2] PFAS mostly have high chemical and thermal stability due to the presence of carbon–fluorine bonds. In addition, the presence of hydrophilic functional groups makes PFASs water soluble despite the hydrophobic nature of their fluorocarbon tail.[3,4] Products that contain PFAS include non-stick glassware, electronics,[5] medical equipment, and fire foaming units.[6,7] Perfluorooctane sulfonic acid (PFOS) and perfluorooctanoic acid (PFOA) are two chemicals that have been considered as the most emerging persistent organic pollutants.[8,9] PFASs have been discovered in the environment as well as in the human body because of their extensive applications and distinctive properties. Studies on PFAS exposure have shown that PFASs can build up in blood tissues and have harmful effects on the

human health such as carcinogenicity and/or immunotoxicity effects.[10,11]

Thus, in the chemical environment that is rapidly changing, environmental health scientists confront a significant difficulty in determining the relative significance of various exposure pathways to PFAS in various human populations and their possible consequences on the human health.[12,13] To ensure public health, efforts have been made to analyze the content of PFAS in drinking water. The detection of PFAS compounds is based on various chromatographic methods coupled with mass spectrophotometry (MS).[14] Although the integration of chromatography with MS technologies offers the most sensitive and precise measurement of PFAS, it is also vital to establish on-site, real-time monitoring systems for PFAS. Therefore, different portable and facile processes have also been investigated for the detection of PFAS in different environments. On April 10, 2024, the U.S. Environmental Protection Agency (EPA) finalized the National Primary Drinking Water Regulation (NPDWR) for six per- and poly-fluoroalkyl substances (PFAS), representing a major advancement in public health protection. Developed after extensive stakeholder engagement and review of over 120 000 public comments, this regulation is expected to safeguard nearly 100 million individuals from PFAS-contaminated drinking water, preventing thousands of fatalities and associated chronic diseases. The NPDWR establishes enforceable maximum contaminant levels (MCLs) for key PFAS, including PFOA and PFOS, and introduces a hazard Index-based

*a*Interdisciplinary Centre for Water Research (ICWaR), Indian Institute of Science, Bangalore, 560012, India. E-mail: onegroupb203@gmail.com

*b*Environmental Science and Industrial Development Department, Faculty of Postgraduate Studies for Advanced Sciences, Beni-Suef University, Egypt

† Equal contribution.

MCL for PFAS mixtures. Complementing these measures, the EPA has defined health-based Maximum Contaminant Level Goals (MCLGs) for selected PFAS. To support nationwide implementation, $1 billion from the Bipartisan Infrastructure Law has been allocated for PFAS monitoring, treatment in public water systems, and remediation assistance for private well owners.[15]

This review examines the sources, occurrence, applications, and exposure pathways of PFAS, alongside their impacts on plants, the aquatic and terrestrial ecosystems, and human health. The detection techniques and recent advances in PFAS removal are discussed, highlighting how parameters such as pH, ionic strength, and solubility influence the remediation efficiency. Furthermore, this review provides a comparative assessment of conventional and emerging treatment technologies including adsorption, membrane filtration, photocatalysis, electrochemical oxidation, and bioremediation, emphasizing their mechanisms, limitations, and scalability. Special attention is given to the transformation behavior and persistence of PFAS during degradation processes, as well as the formation of short-chain intermediates with potential environmental risks. This review also explores policy developments, regulatory frameworks, and risk management strategies aimed at mitigating PFAS contamination, underscoring the importance of integrating advanced analytical tools, sustainable materials, and circular economy principles for the long-term control and remediation of PFAS.

2. Sources, applications, and exposure pathways of PFAS

PFAS have already been recognized as emerging environmental contaminants[16] that tend to bioaccumulate in organs such as the liver, blood and kidney.[17] Therefore, understanding the sources from where PFAS emerge is important. Being a class of human-made organic materials, all the sources of PFAS reported to date are anthropogenic. PFAS tend to emerge in the environment from various anthropogenic sources such as production plants, industrial effluents (metal electroplating plants and textile treatment), fire-fighting foams, and consumer products (cosmetics, food packaging, paints, furnishings, non-stick cookware, carpet, and leather).[18–21] The major sources of PFAS include: (i) manufacturing and industrial facilities; (ii) aqueous film-forming foams (AFFFs); (iii) waste management sites, and (iv) residuals from wastewater treatment plants (WWTPs).

Some manufacturing and industrial facilities constitute the primary source of PFAS by acting as the site of PFAS synthesis, while some manufacturing and industrial facilities utilize PFAS-based materials as a part of their industrial protocol, such as coating of industrial products, constituting secondary sources. However, in both cases, the effluents emerging from the manufacturing and industrial facilities contain PFAS such as PFOA, PFOS, perfluorononanoic acid (PFNA), perfluorohexanoic acid (PFHxA) and perfluorodecanoic acid (PFDA).[22] Accidental spills, leakages, and plume emissions could also lead to the entry of PFAS into the environment.[23,24] PFAS have been manufactured globally, employing processes such as electrochemical fluorination and fluorotelomerization,[25] owing to their numerous applications (Fig. 1). The properties of PFAS such as hydrophobicity, oleo-repellence, thermal stability, friction-decreasing nature, surface active properties, and chemical stability make them a promising class of materials for various applications.[26] PFAS are utilized in the following sectors:
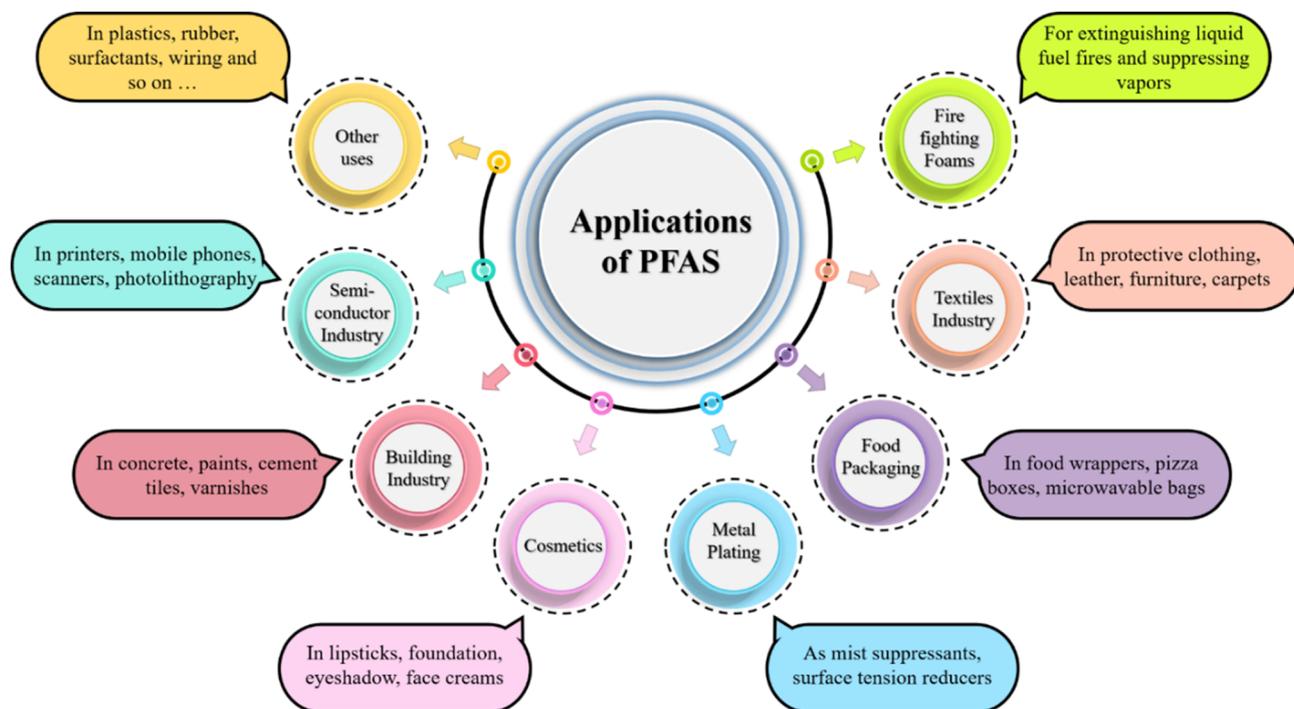

Fig. 1 Applications of PFAS in consumer products.

© 2025 The Author(s). Published by the Royal Society of Chemistry

2.1 Packaging products

Commercial products such as food wrappers, pizza boxes, paper cups, and microwaveable bags are coated with PFAS to prevent the leakage of moisture and oil from foods.[26,27]

2.2 Textile products

PFAS are utilized to treat products such as leather, protective clothing, umbrellas, footwear, carpets, and furniture to prevent them from being damaged by oil, water and stains.

2.3 Semiconductor industry

PFAS are utilized in the fabrication of devices such as mobile phones, scanners, printers, and cameras. Photolithography, an important process in the semiconductor industry, uses PFOS in antireflective coatings.[28,29]

2.4 Construction materials

Materials used in the construction of buildings, such as composite wood, insulation materials, lightweight concrete, paints, house doors, cement tiles, greenhouses, and varnishes, contain PFAS.[26]

2.5 Metal plating

PFOS is used as a mist suppressant to prevent the emergence of toxic fumes during metal plating. Also, PFAS in electrolyte solution reduce its surface tension, and thereby assist the metal plating process.[26,30]

2.6 Other applications

PFAS are utilized in wiring, plastics, rubber, surfactants, industrial equipment such as pipes and reactors, batteries, as well as the aviation industry.[26] Moreover, PFAS are used in cosmetic products such as face creams, eye shadow, lip balms and foundation.[26,31]

Consequently, commercial products act as sources of PFAS in the environment as well as humans. The leaching of PFAS from packaging materials, textiles, and furniture is possible *via* transfer to food and activities involving laundry and cleaning. Hence, alternatives to PFAS have been developed and are being adopted due to the rising concern of PFAS toxicity. However, products made years ago and treated with PFAS are still in use, and therefore cannot be ignored as potential sources of PFAS.

The use of AFFFs containing PFAS in fire safety training sites or during the time of emergency to extinguish liquid fuel fires and suppress vapours lead to the release of PFAS in the environment, especially the soil, and therefore in water bodies.[32–34] Waste management sites such as landfills and scrap yards are the ultimate storehouses for PFAS originating from adulterated industrial effluents, sludge from sewage, and commercial products. PFAS can leach from these areas, thereby entering the soil, groundwater and surface waters.[35–38] WWTPs often utilize conventional water treatment methodologies that do not efficiently remove PFAS. Hence the residuals from WWTPs, such as biosolids and effluents, contain PFAS, which enter the soil, and therefore, aquatic systems such as groundwater and surface water easily.[39,40] Biosolids are also utilized in land applications such as soil modification, which leads to the exposure of soil to PFAS.[41]

The exposure of flora and fauna to PFAS is inevitable (Fig. 2). Once PFAS leach from waste materials, they enter the soil and
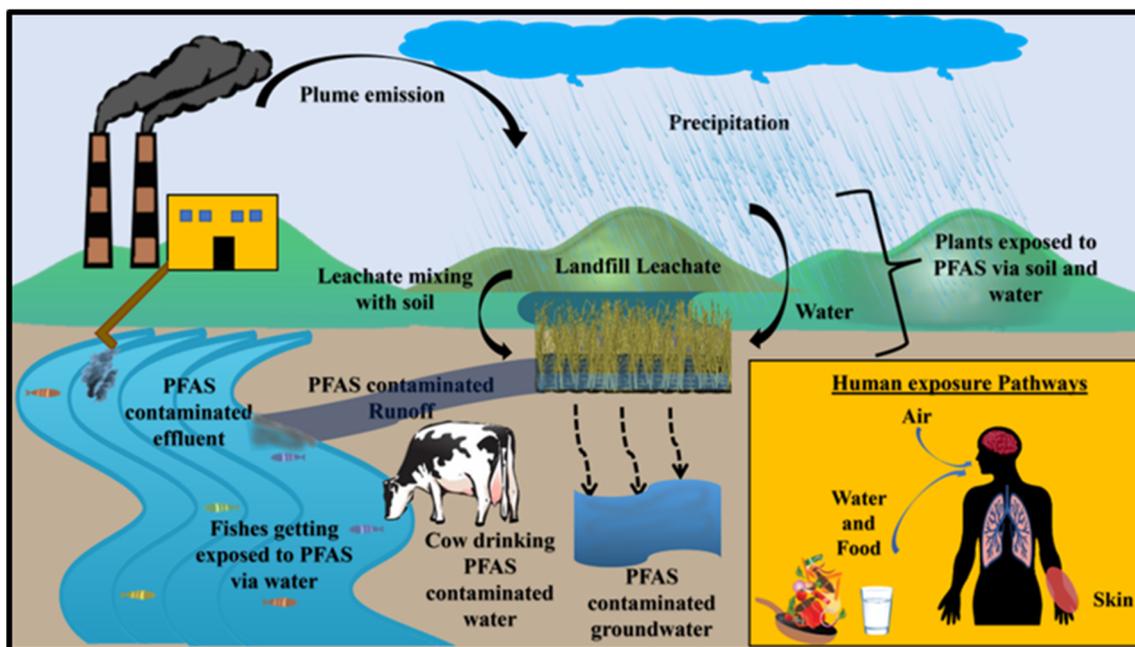

Fig. 2 PFAS exposure pathways to various species.

disturb the growth of plants.[42,43] When PFAS leach from landfills and soil, they reach groundwater and surface water, thereby affecting aquatic animals and plants, as well as terrestrial animals who intake water from these aqueous systems for their survival. The exposure of humans to PFAS is possible *via* various pathways such as air (through inhalation of air contaminated with PFAS),[44] food (through the intake of food contaminated with PFAS leached from non-stick cookware or packaging materials),[45] water (through drinking water contaminated with PFAS)[46] and skin contact (through the utilization of cosmetics containing PFAS or dermal contact arising from PFAS containing products such as water-repellent clothing).[47,48] Among them, water is one of the major pathways by which human beings can get exposed to PFAS. Apart from directly drinking water contaminated with PFAS, indirectly eating seafood that came in contact with water contaminated with PFAS also leads to PFAS exposure through biomagnification in the food chain. Therefore, in this review, the focus is on the remediation of PFAS and methodologies for their detection in water and wastewater.

3. Toxicity of PFAS

In recent years, PFAS, being bioaccumulative and exhibiting toxic effects on the environment, has become a global health concern. PFOA and PFOS, the most widely employed PFAS, have been phased out or banned by several nations of the world. These PFAS have also been listed in the Stockholm Convention on Persistent Organic Pollutants.[49] The half-life of some PFAS has been reported to be more than 92 years in water, which makes them persistent and critically concerning contaminants.[50] Researchers often utilize experimental models such as rats or mice as test species in PFAS toxicity studies. However, alternative models such as zebrafish and *in vitro* cultures are also being explored to investigate their toxicity pathways. These studies typically examine harmful effects related to disturbances in development, reproduction, the immune system, liver, kidney, and carcinogenicity.[51] In addition to animal models, phytotoxicity studies use test species such as lettuce, algae, and wheat to investigate toxic effects on cell morphology, photosynthesis, and growth rate. The pollutants being studied and their respective impacts are detailed in this section and summarized in Table 1.[52] In this section, the toxicity of PFAS to plants, animals (terrestrial and aquatic), and humans is reviewed.

3.1 PFAS toxicity in humans

As mentioned in the previous section, humans can be exposed to PFAS through various pathways, mainly including air, water, food and skin contact. PFAS exposure can be occupational (industrial workers) or non-occupational, and PFAS have been detected in various parts of the human body, such as blood,[76] breast milk,[77] placenta,[78] and hair.[79] The toxicity of PFAS to humans has been linked to several health-related issues such as breast cancer,[80] infertility,[81] vitamin D deficiency,[82] increased cholesterol,[83] diabetes,[84] altered metabolism,[85] thyroid toxicity,[86] atherosclerosis,[87] osteoporosis,[88] and cardiovascular diseases.[61] Individually, various PFAS and their associated health-related issues are summarised in Table 1.

Recent studies have found a correlation between vitamin D deficiency in pregnant women and the concentrations of certain PFAS, including PFDA, PFOS, PFHxS, and *N*-methyl perfluorooctane sulfonamido acetic acid (NMeFOSAA). However, no such correlation was observed with PFAS mixtures.[82] Additionally, indicators of atherosclerosis, such as carotid plaque and echogenicity, were found to be correlated with the concentrations of perfluoroundecanoic acid (PFUnDA) in these women.[87] The thyroid toxicity of various PFAS such as PFOA, GenX and ammonium 4,8-dioxa-3H-perfluorononanoate (ADONA) was investigated by Zhang *et al.*[86] They reported that all three PFAS caused altered gene expression in thyroid cells, with GenX depicting the most disruption effects in the thyroid cells. Further, in a study by Cui *et al.*,[89] male hormonal (such as in testosterone and estradiol) alteration was found to be associated with certain PFAS such as PFOA, PFOS and PFNA. PFAS exposure has also been associated with various types of cancer, such as renal cancer,[90] prostate cancer[91] and ovarian cancer.[92] Roth *et al.*[93] reviewed the risk of type 2 diabetes associated with exposure to PFAS and suggested that a strong testimonial exists to support the link between PFAS exposure and key indicators in diabetes, such as glucose levels and insulin resistance.

3.2 PFAS toxicity in plants

The exposure of plants to PFAS can be considered mainly through the medium of water and soil. The utilization of sewage sludge as a soil modifier[41] is also responsible for the exposure of PFAS to plants. PFAS tend to accumulate in the various parts of the plants, such as leaves, roots, grains, straw, shoots, fruits and stover.[94] The toxic effects of PFAS in plants include improper growth, effect on biomass, perturbed biochemical activities (photosynthesis, metabolism, and gene expression), cell structure damage and inhibited rate of germination.[43,95] In a study by Ebinezer *et al.*,[42] growth effects on the hydroponically grown maize plants upon exposure to PFAS were observed, such as reduced root growth and altered photosynthetic parameters. Significant effects were observed in the photosynthesis parameters such as transpiration rate (+25.8%), photochemistry II (+28.4%), stomatal conductance (+25.8%), and rate of assimilation (+32.3%). A recent hydroponic study by Zhang *et al.*[96] indicated that high concentrations of fluorotelomer sulfonic acid (FTSA), such as 200 µg L^{-1}, can cause adverse effects on the antioxidative defence system of the *Lemna minor* plant by inhibiting the activity of the catalase enzyme. The cytogenotoxicity of PFOS in onion plants was studied by Sivaram *et al.*,[97] which revealed a reduction in the mitotic index, affected cell division and presence of chromosomal abnormalities. They obtained an EC$_{50}$ value of 43.2 mg L^{-1} for PFOS based on the mitotic index. In another study by Li *et al.*,[98] a change in various metabolites such as amino acids, fatty acids, carbohydrates, lipids and antioxidants was reported in lettuce roots upon exposure to PFOS and PFOA in hydroponic media. The distortions in metabolic pathways such as the tricarboxylic acid (TCA) cycle, terpenoid backbone biosynthesis, fatty acid metabolism,

Table 1 Various PFAS and their health-related issues[a]

PFAS	Toxic effects	Human/Animal sample	Reference
PFOS	Metabolite alteration	Blood	53
	Decreased male hormones	Semen	54
	Vitamin D deficiency during pregnancy	Blood	55
	Pancreatic development alteration	Progenitor cells	56
	LDL cholesterol increment	Blood	57
	Total cholesterol increment	Blood	58 and 59
	Glucose homeostasis disruption	Blood	60
	Cardiovascular disease	Blood	61
	Affects liver cells	Liver cells	62
	Epigenetic modification	Non-small cell lung carcinoma cell line	63
	Blood-cerebrospinal fluid (CSF) barrier penetration	Cerebrospinal fluid	64
PFOA	Affects male reproductive health	Semen	54
	Vitamin D deficiency during pregnancy	Blood	55
	Pancreatic development alteration	Progenitor cells	56
	Diabetogenic effect	Blood	65
	Glucose metabolism disruption	Blood	66
	Increased lipid level	Blood	59
	Thyroid toxicity	Thyroid cells	67
	Fasting glucose increment	Blood	57
	Increased lipids in childhood	Blood	58
	Glucose homeostasis disruption	Blood	60
	Epigenetic modification	Non-small cell lung carcinoma cell line	63
	Affects liver cells	Liver cells	62
	Pro-inflammatory cytokine elevation	Blood	68
	Osteoporosis	Blood	69
	Blood-cerebrospinal fluid (CSF) barrier penetration	Cerebrospinal fluid	64
PFNA	Vitamin D deficiency	Human blood	55
PFNA	Affects male reproductive health	Human semen	54
	Insulin and total cholesterol elevation	Human blood	70
	Increased lipid levels	Human blood	59
	LDL cholesterol increment	Human blood	57
	Increased lipids in childhood	Human blood	58
	Affects liver cells	Human liver cells	62
	Osteoporosis	Human blood	69
PFHxS	Infertility	Human ovarian follicular fluid	71
	Vitamin D deficiency	Human blood	55
	Diabetogenic effect	Human blood	65
	Increased lipid levels	Human blood	59
	Increased lipids in childhood	Human blood	58
	Affects liver cells	Human liver cells	62
PFDA	Insulin and total cholesterol elevation	Human blood	70
	Increased lipids in childhood	Human blood	58
	Affects liver cells	Human liver cells	62
	Dental decay	Human blood	72
PFBS	Increased childhood adiposity	Umbilical cord blood	73
GenX & ADONA	Thyroid toxicity	Thyroid cells	67
PFMOBA	Impairment of development and locomotory function	Zebrafish embryo	74
PFDMMOBA & PFO2DA	Impairment of development and locomotory function	Zebrafish embryo	74
GenX	Shifts in the metabolic profile	Daphnia magna	75
PFBA	Glucose homeostasis disruption	Human blood	60
	Osteoporosis	Human blood	69
Cl-PFESA	Affects male reproductive health	Human semen	54
	LDL cholesterol increment	Human blood	57
	Glucose homeostasis disruption	Human blood	60
	Blood-cerebrospinal fluid (CSF) barrier penetration	Cerebrospinal fluid	64

[a] PFOS – perfluorooctane sulfonate, PFOA – perfluorooctanoic acid, PFNA – perfluorononanoic acid, PFHxS – perfluorohexane sulfonate, PFDA – perfluorodecanoic acid, PFBS – perfluorobutane sulfonate, GenX – hexafluoropropylene oxide dimer acid (HFPO-DA), ADONA – ammonium 4,8-dioxa-3H-perfluorononanoate, PFMOBA – perfluoro-3-methoxypropanoic acid, PFDMMOBA – perfluoro-4,7-dioxa-5-methyl-8-methoxy-octanoic acid, PFO2DA – perfluoro-2,7-dimethyl-3,6-dioxaoctanoic acid, PFBA – perfluorobutanoic acid, and Cl-PFESA – chlorinated polyfluoroether sulfonic acid.
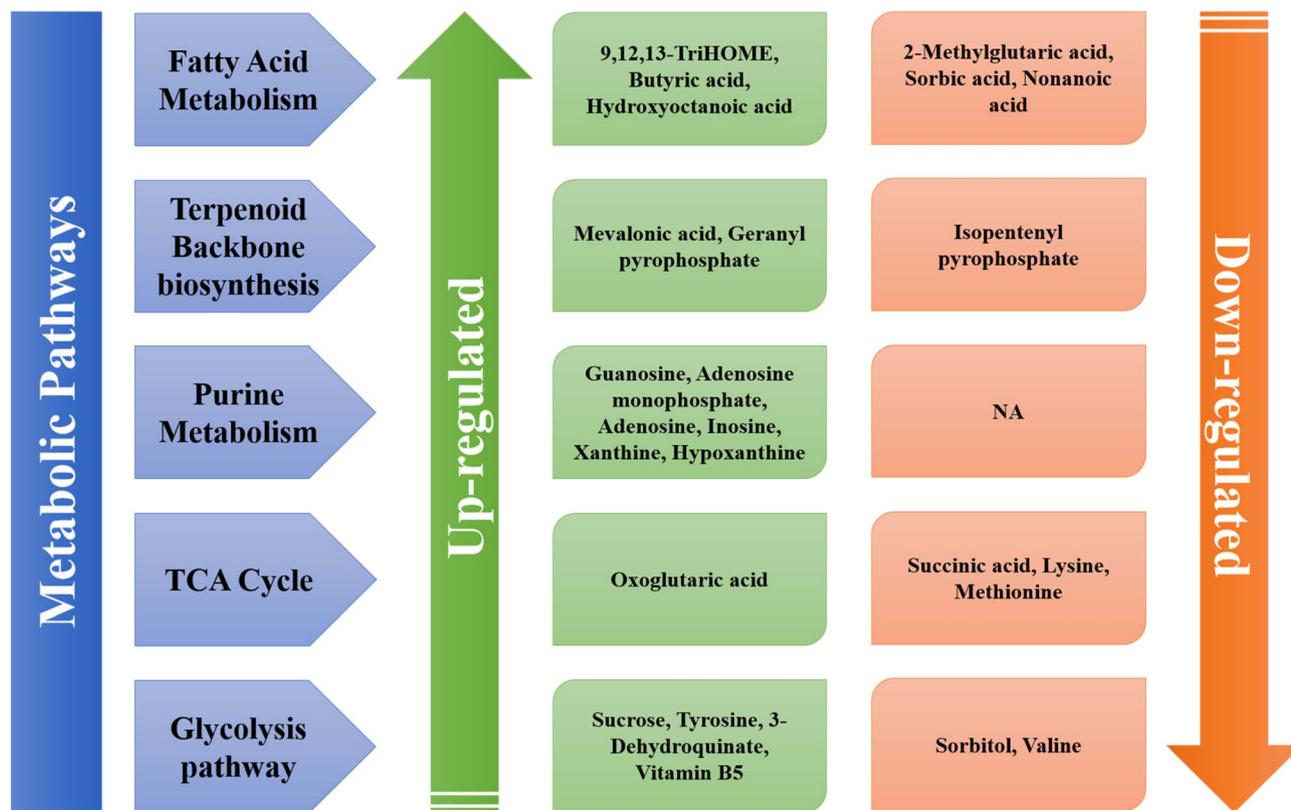
RSC Advances

Review

Fig. 3 Distortions in the metabolic pathways of lettuce roots upon PFAS exposure.

glycolysis, and purine metabolism in the lettuce roots are illustrated in Fig. 3.

3.3 PFAS toxicity in animals

3.3.1 Terrestrial animals. The exposure of terrestrial animals to PFAS, as discussed earlier, is mainly possible through the water and soil. PFAS has been detected in the serum and organs of various animals. For instance, PFOS and PFHxS have been detected in the serum of cattle[99] and cats.[100] PFOS has been detected in the liver of sheep feeding on contaminated grass.[101] Further, PFCAs and PFOS have been detected in tissue samples such as the liver and muscle of dairy cows.[102] The toxicity of PFAS towards terrestrial animals has been linked with altered metabolism,[103] alteration in insulin secretion,[104] alteration in dopamine levels,[105] immunotoxicity,[106] neuronal toxicity,[107] altered gene expression,[103] and hormonal imbalance.[108] A study by Jacobsen et al.[103] revealed an alteration in the gene expression involved in the metabolism of lipids in the developing embryos of chicken upon exposure to PFOS. They observed the downregulation of the FABP7, ACSL6, ACAD8 and ELOVL3 genes in both 1.0 and 0.1 μg g^{-1} of the PFOS treatment groups. Recently, the immunotoxicity effects of PFOA and PFOS on mice upon exposure to AFFFs via drinking water were reported by McDonough et al.,[106] wherein suppression in the responses of SRBC-specific IgM antibody was observed.

3.3.2 Aquatic animals. Aquatic animals get exposed to PFAS mainly through effluents containing PFAS entering the

aquatic systems. PFAS have been detected in various aquatic creatures such as *Channa argus*, *Hypophthalmichthys molitrix* and *Cyprinus carpio*.[109] PFAS such as PFDA, PFDoA, PFUnA and PFOS were detected in the tissues of mandarin fish.[110] The toxic effects of PFAS among aquatic animals include immune dysfunction,[111] behavioural abnormalities,[112] altered liver function,[111] metabolic alteration,[113] thyroid toxicity,[114] and malformation of offspring.[115] In a study by Shi et al.[115] endocrine disruption effects and malformation in offspring were observed in zebrafish upon co-exposure to alternatives to PFOS, such as FTAB and FTAA, at concentrations of 500 and 50 μg L^{-1}, respectively. In another study by Soloff et al.,[116] exposure to PFOS in dolphins led to dysregulation of their cellular immune system. They also observed an enhancement in CD4$^+$ and CD8$^+$ T cell proliferation upon exposure to PFOS. The toxicity of per-/poly-fluoroethers carboxylic acids (PFECA) investigated by Gebreab et al.[117] on zebrafish embryos revealed distorted metabolism profiles similar to the toxicity of PFOA. They calculated the LC$_{50}$ value of PFECA (such as GenX) and PFOA as 383 ± 30 and 232 ± 29 μM, respectively. Recently, thyroid toxicity was explored via modelling as well as in vivo studies by Chen et al.[114] in the zebrafish embryos due to exposure towards diPAP.

Considering the toxic effects of PFAS on various species in the environment (Fig. 4), and water being one of the major exposure pathways to various species, it is critical to effectively detect and remediate these anthropogenic contaminants via
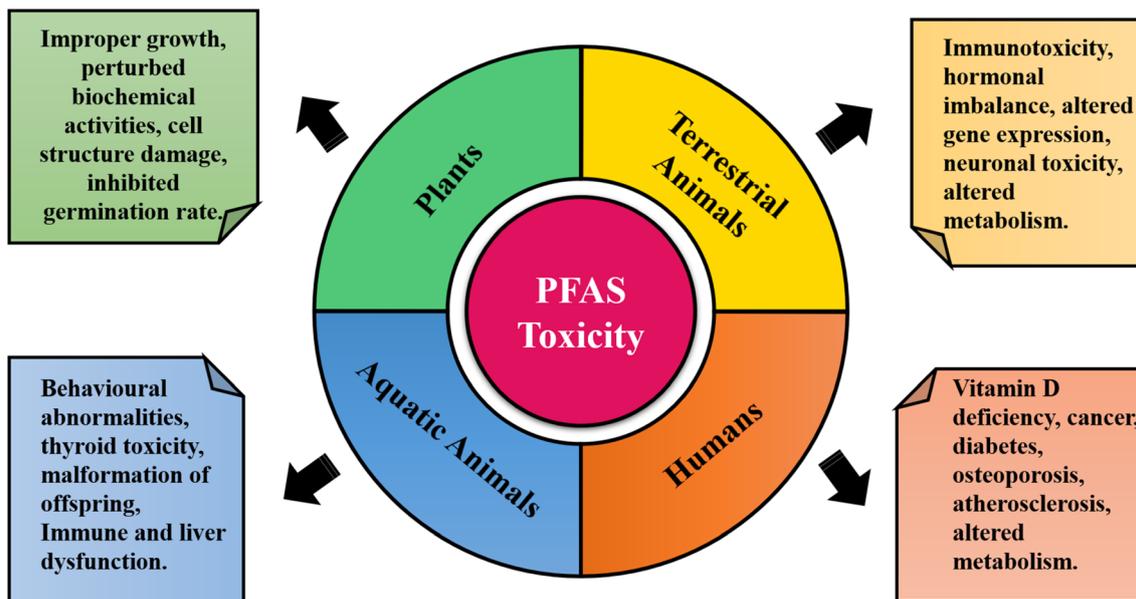
Fig. 4   PFAS toxicity to various species.

UHPLC-MS/MS. Therefore, in the upcoming sections, the detection and remediation methodologies for PFAS have been extensively reviewed.

4. Analytical detection and quantification of PFAS in water and wastewater

Multiple analytical techniques have been employed for the detection of PFAS across water, soil, sediment, and biological matrices. Methods such as LC-MS/MS, PIGE, TOP assay, EOF, and NMR provide complementary insights into the concentration, speciation, and precursor transformation of PFAS, enabling comprehensive environmental and biological assessment.[118]

4.1 Solid-phase extraction

The solid-phase extraction (SPE) method is used to pre-concentrate PFAS analytes in water prior to their further analysis such as high-performance liquid chromatography integrated with tandem mass spectrometry (HPLC-MS) to lower the overall method limit of quantification (MLQ). For example, it has been effectively used to extract PFAS ($C > 4$), where styrene divinylbenzene and weak anion exchange (WAX) resins have been used. In particular, tri-fluoromethanesulfonate (TFMS), PFBS, and a number of PMOCs have been shown to be responsive to WAX-based SPE techniques. The results demonstrate that in addition to TFMS and PFBS, WAX SPE could also successfully extract 2-ACO-DFEtS and 10-CS. The concentration of each target analyte in solution was created by adding analyte standards to ultrapure (Milli-Q) water for SPE testing utilizing Oasis WAX. The anionic character of the analytes and their affinity for the WAX resin are constant. This is especially true for TFMS, which may be the most hydrophilic PFAS molecule. The MLQ values of HPLC-MS following SPE ranged from 0.02 to

0.06 ng L^{-1} when using the Oasis WAX cartridges, drastically decreasing the detection limit of the technique as shown in Fig. 5.[119] However, the main limitation of this method is the interference from suspended particles in water, which requires an extra filtration step. Also, much more development and validation are required.

Twelve PFAS were found in surface water after being extracted with SPE cartridges, and then analysed with HPLC. PFHxA (1.5–187.0 ng L^{-1}), perfluoropentanoic acid (below detection limit [BDL] of 169.9 ng L^{-1}), PFOA (BDL of 65.5 ng L^{-1}), and perfluorobutane sulfonic acid (BDL of 44.7 ng L^{-1}) were the most common PFAS species.[121]

Online solid-phase extraction (SPE) utilizing weak anion exchange is employed to concentrate samples, enhancing the
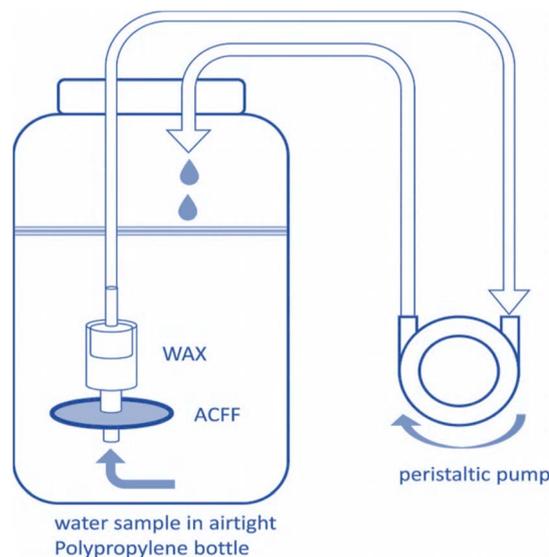

Fig. 5   Schematic of the *in situ* SPE set-up.[120]

sensitivity and removing matrix interferences. This technique is suitable for detecting perfluorocarboxylates (C4 to C12), perfluorosulfonates (C4 to C10), HFPO-DA, and some fluoro-telomer sulfonates. To analyze other PFAS analytes, such as alkylated sulfonamides and other uncharged compounds, alternative sorbent techniques such as hydrophobic sorbents may be necessary.[122]

4.2 Isotope dilution

Isotope dilution relies on the addition of a carefully measured quantity of a highly enriched isotope to a sample, changing the isotopic content in the target element. The mass fraction of the target element in the sample can be determined by measuring the modified isotopic composition of the element.[123] This method is flexible and can be integrated with other techniques for the analysis of different PFAS. For example, isotope-dilution integrated with LC/MS/MS is typically utilized to quantify the concentration of PFAS in water. This technique allows the correction of PFAS adsorption losses by using surrogate recovery standards and stable isotope internal standards, which are applied to the sample bottles prior to sample collection. The generation of laboratory waste significantly decreases because of the use of stable isotopes and direct sample injection onto the LC apparatus, and the analytical precision increases.[124] Isotope dilution tandem mass spectrometry integrated with UPLC is implemented to limit the range of sulfonamide, carboxylate, and sulfonate PFAS analytes from 0.25 to 4000 ng L^{-1}. Fig. 6 presents the procedure for the standard method of isotope dilution implemented in U.S. EPA.

Isotope dilution is also coupled with SPE-LC/MS/MS to detect new chemical structures of PFAS with a detection limit in ng L^{-1} or ng kg^{-1} (ASTM) such as PFUnA (2.7 ng L^{-1}), PFPeS (6.3 ng L^{-1}), PFPeA (3.9 ng L^{-1}), PFOA (3.4 ng L^{-1}), PFOS (4.4 ng L^{-1}), 6 : 2 FTS (14 ng L^{-1}), PFHpA (2.6 ng L^{-1}), 8 : 2 FTS (9.1 ng L^{-1}), PFBS (3.5 ng L^{-1}), PFDA (2.3 ng L^{-1}), NFDH (16 ng L^{-1}), PFDoA (2.2 ng L^{-1}), PFBA (13 ng L^{-1}), PFHxS (3.7 ng L^{-1}), 4 : 2 FTS (4.7 ng L^{-1}), PFHxA (5.3 ng L^{-1}), PFHpS (5.1 ng L^{-1}), PFEESA (2.6 ng L^{-1}), PFMPA (3.8 ng L^{-1}), PFMBA (3.7 ng L^{-1}), PFNA (4.8 ng L^{-1}), 9Cl-PF3ONS (1.4 ng L^{-1}), and HFPO-DA (3.7 ng L^{-1}).[126]

4.3 Liquid chromatography/tandem mass spectrometry (LC/MS/MS)

Liquid chromatography/tandem mass spectrometry is a common technique that has been widely applied to detect PFAS in water and wastewater. However, researchers are working on the development of this method. For example, the development, validation, and application of a straightforward and reliable analytical method based on solid-phase extraction and LC-MS/MS for the detection of perfluorinated carboxylic acids (PFCAs) with C2 to C8 chains in tap, ground, and surface waters. Two materials with weak anion-exchange characteristics for SPE (Oasis WAX and Strata X-AW) and two stationary phases for LC (Kinetex C18 and Obelisc N) were also assessed. The reversed phase column with an acidic eluent produced robust separation and retention. In the case of PFCAs with $C > 3$, quantitative extraction recoveries were often attained; however, the extraction efficiency varied for the two shortest chained analytes. Specifically, with Strata X-AW, between 36% and 114% of perfluoropropanoate (PFPrA) and 14% and 99% of trifluoroacetate (TFA) were recovered, while Oasis WAX recovered 93% to 103% of PFPrA and 40% to 103% of TFA. It was determined that the sample pH was a crucial factor in the extraction procedure. To reduce the sample preparation steps and eliminate sorbent particles, one-step elution-filtration was added to the workflow. The limit of quantitation (LOQ) for all PFCAs ranged from 0.6 to 26 ng L^{-1} because of validation. The precision ranged from 0.7% to 15%, and the mean recoveries were between 83% and 107%. The PFCA values ranged from 0.056 to 2.2 g L^{-1} in groundwater samples taken from areas where PFASs had been present. The two main analytes were TFA and perfluorooctanoate. However, TFA showed a wider distribution and was discovered in drinking water and groundwater in quantities between 0.045 and 17 g L^{-1}.[127]

A liquid chromatograph has been connected to a triple quadrupole mass spectrometer in a proposed approach, which only requires that the sample be filtered. Strong matrix effects were discovered for some of the target PFASs, and matrix-matched calibration curves were recorded to enable precise (%RSD between 3% and 18%) and accurate (87–114%) quantification ($n = 5$, at 5 and 75 ng L^{-1}), with excellent sensitivity (LOQ between 0.1 and 2.0 ng L^{-1}). The technique was used on water samples from tap water and bottled water, as well as influent and effluent from a drinking water treatment facility in Catalonia, Spain. PFBA, which made up 69%, 66%, 49%, and 48% of all the PFASs identified in bottled, tap, effluent, and influent waters, respectively, was the most prevalent PFAS across all forms of water. The total mean concentrations in the influent and effluent water as well as relative mean abundances point to subpar PFAS removal during drinking
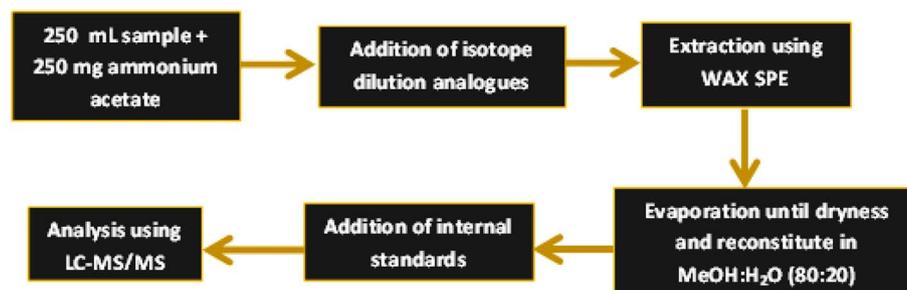

Fig. 6 Steps of the U.S. EPA Method-533 implemented isotope dilution.[125]

© 2025 The Author(s). Published by the Royal Society of Chemistry

water treatment. In general, tap water had higher PFAS contents than bottled water.[128]

4.4 High-performance liquid chromatography

High-performance liquid chromatography (HPLC) is an advanced version of liquid chromatography (LC), which operates at significantly higher pressures than standard LC. Although conventional LC relies on gravity to move the mobile phase through the column, resulting in a slow flow rate and limiting the size of particles that can be used, HPLC uses pumps to propel a pressurized liquid through the column. This approach significantly reduces the separation time and enhances the efficiency. The smaller stationary particles used in HPLC columns compared to those in regular LC provide a higher resolving power, allowing the better separation of mixtures. For example, 250 mL of contaminated water is strengthened with surrogates and flow through an SPE cartridge, which contains polystyrene divinylbenzene to efficiently separate the PFAS chemicals from the aqueous media. A small amount of methanol is used to extract PFAS from the solid-phase adsorbent in the water sample to accurately detect the PFAS in the sample.[118] The general procedure for the detection of PFAS using HPLC is illustrated in Fig. 7.

HPLC was used to detect different types of persistent PFAS precursors, transformed intermediates, and newly found PFAS in water discharged from wastewater treatment plants. For example, HPLC was implemented to detect the sum of fluorotelomer sulfonic acids with a concentration of 0.8–1.3 ng g^{-1}. The detected perfluorooctane sulfonamides and ethanols ranged from 0 to 3.2 ng g^{-1}, and the sum of polyfluoroalkyl phosphoric acid esters was 15–20 ng g^{-1} dry weight. PFSAs and PFCAs were found at concentrations of 1.9–3.9 ng g^{-1} and 2.4–7.3 ng g^{-1} dry weight, respectively. The bulk of the persistent PFCAs and PFSAs in water was found to significantly increase after wastewater treatment, providing further evidence of the influence of the precursor chemicals. Perfluorooctane sulfonic acid, perfluorohexane sulfonic acid, PFOA, and PFHxA experienced a net mass increase with mean values of 58%, 37%, 28%, and 83%, respectively, in wastewater treatment plants.[129]

Using HPLC-MS/MS analysis, the concentrations of 19 PFAS in surface and ground waters were found to be 66.2 185 ng L^{-1} and 44.8–209 ng L^{-1}, respectively. The analytes were extracted using SPE-Strata X-AW cartridges, combined with ultrasonication treatment using methanol and deionized water, resulting in excellent recovery rates of 81–130%. Similarly, short-chain PFCAs (C2–C8) were detected in tap, ground, and surface waters.[131] Prior to SPE with OASIS HLB cartridges, dual filtering (cellulose membrane and glass microfibre filter GF/A) has been used as a pre-treatment procedure.[132] Quantifying short, long, legacy, and emergent PFAS in surface water from various places was done quickly.[133] To monitor PFAS (C5–C17), HPLC coupled to ultrahigh resolution Orbitrap mass spectrometry (HPLC-uHRMS) has been described. Samples were taken from wastewater utilizing a C18 sorbent and an online SPE. The estimated method detection limits were 0.005–0.2 ng mL^{-1}.[134] In comparison to off-line pre-treatment procedures, this method is not only faster and more reliable, but also extremely sensitive.[135] Also, HPLC has been used to detect targeted PFAS in a groundwater aquifer utilized for drinking water production. The PFAS concentration in groundwater, river and drinking waters was 1000, 15 ng L^{-1} and varied from 1 to 8 ng L^{-1}, respectively. The low concentration of PFAS in drinking water is attributed to the treatment in the water treatment plant. This refers to the significance of detecting PFAS in different water resources to record the variations in the concentration of PFAS during transportation from polluted resources and their subsequent impact in the resulting drinking water to directly identify PFAS in ambient water samples without first concentrating the samples. Centrifugation of the samples followed by filtration was implemented, followed by
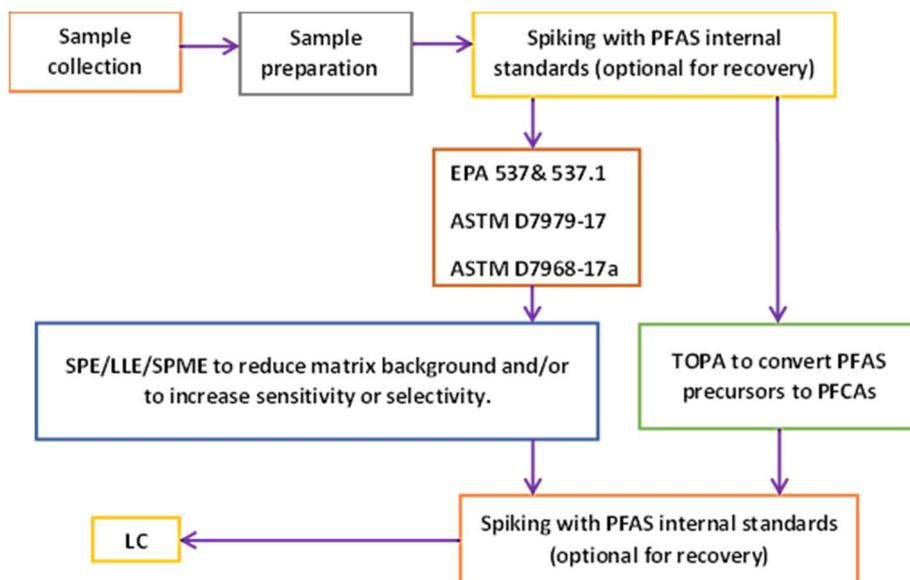

Fig. 7 Schematic flow diagram for the general procedure of PFAS analysis using LC.[130]

analysis using UPLC-MS/MS utilizing an AB Sciex 6500 with Q-Trap mass spectrometer in a negative multiple reaction-monitoring (MRM) mode after the addition of ammonium acetate. To reduce interference from background PFAS, the instrument system adds a delay column between the pumps and autosampler. This approach tracks eight short-/long-chain PFAS, which are identified by tracking the precursor product ion pairs by their retention durations, which are then measured using calibration plots based on isotope mass-labeled internal standards. The average spiking recoveries for the target analytes ranged from 84% to 110% with a 4–9% relative standard deviation (RSD). The mean spiking recoveries of the four surrogates ranged from 94% to 106% with an RSD of 3–8%. The average spiked recoveries for the target analytes for continuous calibration verification (CCV) varied from 88% to 114% with 4% to 11% RSD and from 104% to 112% with 3% to 11% RSD for surrogates. The matrix spike (MX), matrix spike duplicate (MXD), and field reagent blank (FRB) recoveries satisfied the acceptance standards. The limit of detection of the target analytes ranged from 0.007 to 0.04 ng mL^{-1}.[136]

Several trials have been carried out to modify the HPLC-MS/MS. For example, Ice Concentration Linked with Extractive Stirrer is coupled with the HPLC-MS/MS to facilitate the analysis of ultratrace 14 PFAS in drinking water. This technique required only 50 L of methanol for each sample, had an automated extraction process, required only a small sample amount (10 mL), and had little matrix effect. This approach generated good accuracy and precision (*i.e.*, 87% to 108% accuracy and 19% relative standard deviation as a measure of precision) as well as a wide linear range of 0.5 to 500 ng L^{-1} and ultratrace limit of detection (0.05 to 0.3 ng L^{-1}). Fifty two out of the fifty-three samples tested using this approach included at least one PFAS chemical. The maximum concentrations of PFHxA, PFOA, and perfluoroheptanoic acid (PFHpA) were 268, 213, and 75.7 ng L^{-1}, respectively. Additionally, at least one sample of drinking water included PFOA, perfluorodecanoic acid, and PFHpA acid, which were all greater than 20 ng L^{-1}. This technology is readily available and enables ultratrace PFAS detection, while avoiding many of the drawbacks of existing techniques.[137]

4.5 Ultra-high performance liquid chromatography

In HPLC, the stationary phase typically consists of particles measuring 3–5 μm in size. In contrast, ultra-HPLC (UHPLC) utilizes particles that are 2 μm or smaller. The UHPLC columns are also designed with an internal diameter of 2.1 mm or less and are significantly shorter, often around 100 mm in length, compared to HPLC columns, which usually have an internal diameter of 4.6 mm and length of 250 mm. UHPLC operates at much lower flow rates, ranging from 0.2 to 0.7 mL min^{-1} compared to that of HPLC of 1 to 2 mL min^{-1}.

To evaluate PFAS pollution around highly contaminated sites, SPE was used to extract, purify, and pre-concentrate water samples prior to detection using ultra-HPLC linked to tandem mass spectrometry in negative electrospray ionisation mode for the analysis of 29 PFAS, including perfluoroalkyl sulphonic

acids, perfluorocarboxylic acids, and fluorotelomers (FTs), such as sulphonamide betaine, saturated carboxylic acid, sulphonate, unsaturated carboxylic acid, and sulphonamide. Twelve internally labelled standards were employed to create a sufficient correction that would account for matrix effects. Depending on the analytes, the LOQ for water ranged from 4 to 10 ng L^{-1}. To determine the presence of PFAS compounds that are not targeted, a surrogate parameter technique based on the carboxylation of perfluoroalkyl acid precursors under basic pH conditions was also put into practice.[138]

4.6 Total organic fluorine

The total organic fluorine (TOF) method is based on the burning of the entire sample, including all fluorine-containing components, to produce a single fluoride anion, which is then analyzed using a variety of techniques. This technique offers considerable potential for the quantitative determination of fluorine. However, it leads to a total loss of knowledge regarding the structure of the precursors. This means that the contribution from other fluorine sources, such as fluoride itself, non-polyfluorinated organic substances with isolated fluorine atoms, organic substances with SeF or PF bonds, fluoro-aromatic substances, or naturally occurring fluoroorganic compounds could be significant. Extracted organic fluorine (EOF) is a modification of TOF. In EOF, the material is first extracted using an organic solvent, and then the extract is subjected to TOF analysis.[139]

Inductively coupled plasma-mass spectrometry (ICP-MS/MS), X-ray photoelectron spectroscopy (XPS), and fluorine-19 nuclear magnetic resonance spectroscopy (19F-NMR) have all recently been developed for the detection of fluorine and organic fluorine. Once PFAS have been distinguished from the background, such as by SPE, the proton induced gamma emission (PIGE) method can swiftly quantify TOF. In other words, sample preparation affects TOF. The TOF is then measured after extractable fluorinated compounds are adsorbed by adsorbent materials.[130]

Adsorbable organic fluorine (AOF) is an analytical technique involving loading commercially available synthetic polystyrenedivinylbenzene-based activated carbon (AC) with organofluorine compounds, followed by examination of the loaded AC *via* hydropyrolysis combustion ion chromatography (CIC). The excess nitrate produced during extraction and washing the loaded AC with an acidic sodium nitrate solution displace inorganic fluorine. The AOF concentrations produced by the identified PFAS in each sample are calculated using the individual recovery of each PFAS found.[140] These individual yields are determined in ultrapure spiked water, as it is impossible to use wastewater due to the very high concentrations of other PFAS and the potential presence of PFAS with unknown chemical structures. By comparing these calculated values to the measured concentrations of AOF, a percentage of unidentified PFAS is inferred for each sample. Moreover, the AOF in surface, municipal, ground waters and industrial wastewaters has been determined using a rapid, robust, and cost-efficient CIC method. The concentrations of AOF in surface

water, wastewater discharges and ground water were 2.3–24.5 $\mu g\ L^{-1}$, <2.0–8.5 $\mu g\ L^{-1}$, and <2.0 $\mu g\ L^{-1}$, respectively. Compared to LC-MS/MS, an AOF concentration up to 555 $\mu g\ L^{-1}$ was detected, while the individual PFAS in the form of fluorine were recorded to be 8.8 $\mu g\ L^{-1}$. It can be concluded that CIC can detect numerous fluoroorganic substances, which are not detected by LC-MS.[141]

4.7 Total oxidizable precursors assay (TOPA)

Nearly 5000 PFAS are thought to exist in total on the global market. However, 90% of them are categorized as PFAS precursors. Consequently, it is crucial to find PFAS precursors in various matrices. Due to the lack of standards or because the structure of the precursors is unknown, the present detection methods can only identify certain types of PFAS and not their precursors. TOPA, which was developed to analyse PFAS precursors, was created to close this gap. To produce detectable PFAS, such as PFCAs, in TOPA, an excessive amount of oxidant is employed to oxidise the PFAS precursors in an alkaline environment.[130] Strong oxidants such as persulfate and hydroxyl radicals produced during the thermolysis of these substances are some of the oxidants. As a result, TOPA is followed by quantitative analysis. The total oxidizable precursor assay (TOPA) is based on the mild oxidation of non-fluorinated parts of the precursors and their conversion to perfluorocarboxylic or per-fluorosulfonic acids, followed by their analysis by target PFAS methods.[139] When the target PFAS are known, the total oxidizable precursor test is a valuable tool for the detection of PFAS. This approach is only applicable to substances that can undergo oxidation to produce certain PFAAs. A significant benefit of the total oxidizable precursor test is that the detection limit for the precursor of PFOS or PFOA is approximately 1.0 $ng\ L^{-1}$. The entire oxidizable precursor technique is limited to species that are known to be present in water samples.[118]

Houtz and Sedlak[142] originally developed this technique to identify N-methyl fluorooctane sulphonamide, N-ethyl fluoro-octane sulphonamide, and perfluorooctane sulphonamide precursors in stormwater. After the development of TOPA, an increase in the concentration of PFCAs (69%) has been found. One must consider the entire PFAS family, including the PFAS precursors, "knowns" and "unknowns" when assessing the risk and remediating PFAS-related issues. Thus, research efforts have been expanding to enhance TOPA technology and address PFAS and precursors.[142]

PFAS analysis is challenging due to their trace-level presence and the occurrence of unknown precursors that may partially degrade or lack analytical standards. Consequently, advanced techniques such as time-of-flight (TOF) analysis have been developed to improve the detection, identification, and quantification of fluorinated compounds in complex environmental matrices.

4.8 Remote sensing approach for the detection of PFAS

PFAS have been recently categorized as hazardous constituents that can be found in various aquatic habitats.[143] PFAS have been found in frequently used consumer products such as lubricants, paints, ski wax, firefighting foams, polishes, metal plating, outdoor textiles, food packaging, some baking papers, and leather samples. The most widely adopted technique for the qualitative analysis of soil or water samples is in situ sample collection, followed by subsequent laboratory analysis. However, although these conventional techniques are accurate for point locations and a specific time, they are inadequate and disproportionate for spatiotemporal variation assessment.[144] Thus, to fill these gaps in spatiotemporal data resolution, various remote sensing platforms are used, which are categorized as follows: (i) air-borne (aerial photographs and unmanned aerial vehicles) and (ii) space-borne (optical, thermal, hyperspectral, and microwave satellite imageries). Aerial photographs provide good spatial resolution, but their implementation is restricted by the logistical costs associated with planning and execution of aerial flight and the extent of spatial coverage.[145] Space-borne remote sensing datasets acquire frequent and synoptic views of both terrestrial and aquatic ecosystems at sustainable cost. A fundamental principal that governs remote sensing is that each earth surface feature interacts in a different manner with specific wavelengths of the electromagnetic spectrum.[146] Optical satellite datasets, corresponding to the wavelength range of 0.36 μm-2.36 μm are feasible for the determination of water and soil pollutants.[147]

Many studies have investigated the applications of remote sensing images for the assessment of physical and biological soil and water quality parameters thus far. With the advancement in space technologies, various agencies initiated different satellite missions for retrieving estimates of the CO, CO_2 and CH_4 concentrations, as follows: (i) Scanning Imaging Absorption Monitoring Spectrometer for Atmospheric Chartography (SCIAMACHY), Infrared Atmospheric Sounding Interferometer (IASI), and Tropospheric Monitoring Instrument (TROPOMI) were developed by the European Space Agency (ESA), (ii) Greenhouse Gases Observing Satellite (GOSAT) is operated by the Japanese Aerospace Exploration Agency (JAXA), and (iii) Orbiting Carbon Observatory 2 (OCO-2) and Atmospheric Infrared Sounder (AIRS) are operated by National Aeronautics and Space Administration (NASA). There is a dire need to develop satellite missions for the monitoring and evaluation of PFASs to enable the detection of these substances as soon as they appear near the source of contamination.

5. Techniques for the removal of PFAS

The traditional techniques for the treatment of water and wastewater produce waste containing PFAS, which are highly stable and resistant to typical degradation processes. Reverse osmosis (RO), ion exchange, and adsorption into granular activated carbon (GAC) are often employed in the removal of contaminants from drinking water. Compared to drinking water, sludge and biosolids from WWTPs consist of a significant concentration of PFAS.[12] To break down PFAS from wet sludge, various techniques have been developed. The most used method is incineration,[148] but in the case of wet sludge,

Table 2 Efficiencies of various removal techniques for PFAS removal from environmental matrices using different materials

Technique		Method	Removal efficiency (%)	Reference
Membrane process	Absorption	Silane + aluminum oxide hydroxide	90	158
		Polyamide + piperazine	90	159
		Silane with aluminum oxide hydroxide membranes + poly(ethylene glycol)	99.9	158
		β-lactoglobulin amyloid fibril	96	160
		Functionalized graphene oxide	74	161
		Metal–organic frameworks (MOF)	98.4	162
		MXene-polyamide-PS	98	163
		MXene-tannic acid	99	164
		Polyether ether ketone (PEEK)	99	165
	Nano-filtration	NF membrane (ESNA1-K1)	97.9	166
		NF270	98–99	167 and 168
		Polyamide layer + bipiperidine	90	159
	Reverse osmosis	Polyamide (ESPA3 and LFC3)	99	169
		RO membrane (TW30-1812-100)	98.7	170
		Cellulose acetate + polyamide	99.9	171
Absorption		Activated carbon/Biochar	98	172 and 173
Anion exchange		Commercial resins	90–95	174 and 175
Advanced oxidation process		Persulfate activation	97–99	176–178
		Photo-catalytic oxidation	75–100	179 and 180
		UV/sulfite	95	181
		Electron beam	77–97	182 and 183
Biological process			60–80	184 and 4

microwave heating techniques could only break down PFOA by around 50% within a period of four hours. Thermal treatment methods also use lime addition to remove PFOS at extremely severe temperatures between 300 °C and 900 °C.[149] However, although these treatments are successful, their main drawback is the exorbitant energy required to dry wastewater sludge with a high moisture content (>80%) before incineration. To remove PFAS in water/wastewater, two separate strategies can be employed, in which either PFAS are broken down (destructive methods) or removed (non-destructive methods). The various destructive methods for eliminating PFAS from biosolids are pyrolysis,[150] hydrothermal liquefaction (HTL),[151] thermal hydrolysis, and supercritical water oxidation.[152] Different destructive processes, such as photochemical oxidation,[153] direct photolysis,[154] activated persulfate-oxidation,[155] photocatalytic-oxidation, subcritical water, sonochemical decomposition, and electrochemical oxidation[156] are used to remove PFAS from wastewater. Membrane separation, nano-filtration, reverse osmosis, adsorption onto GAC, and ion exchange are effectively used to degrade PFAS from drinking water. The high hydrophilicity and low quantities of PFASs make them unsuitable candidates for removal by traditional coagulation, flocculation, and sedimentation methods.[157] This section describes the PFAS treatment techniques for water and wastewater. Table 2 summaries the removal efficiency of each technique.

5.1   Membrane process

PFAS removal from aqueous streams has been extensively explored using membrane-based methods. Adsorption-based membranes, reverse osmosis (RO) and nano-filtration (NF) are the frequently used membrane methods for the rejection of PFASs. However, their rejection rate may be influenced by fouling and demands high energy/pressure to accomplish the optimal separation. This section explores existing membrane-based methods for the removal of PFAS that are presently on the market.

5.1.1   Absorption-based membranes. Organic polymers are commonly used to manufacture the membranes used for water treatment due to their toughness and easy processing technique. Polyamide (PA), thin film composite (TFC), and poly-carbonate (PC) membranes make up most of the commercial RO and NF membranes used to remove PFAS from water.[185] Johnson *et al.*[158] functionalized fluorinated silane with aluminium oxide hydroxide membranes for the absorption of PFOA and PFOS with an initial concentration of 0.39 ng L^{-1} and 0.86 ng L^{-1}, respectively. The per-fluorinated side chains get absorbed onto the surface, which form C–F interaction, and 90% removal rate was obtained. The optimized conditions are pH 7.5, filtration time of 30 min, and pressure of 0.317 bar. To improve the removal rate, PEG was used, which enhanced the removal rate by 99.9%. Trimesoyl chloride (TMC)-piperazine (PIP) PA membranes have been used for the filtration of PFASs using the NF process. These membranes are hydrophilic surfaces, which improve the antifouling capabilities on the surface. The pores size of the PIP membrane ranges from 0.8 to 2 nm, which inhibits the movement and has high retention for PFOA. Due to the deformed shape of the PIP molecules, the TMC-PIP layer typically has pores that are between 0.8 and 2 nm in size on average. High retention of PFOA (~90%) has been recorded.[159] PFSAs and PFCAs have been retained using a β-lactoglobulin amyloid fibril membrane with a removal rate of

96%.[160] Nano-porous polyamide, which increased the surface charge of the membrane to negative, has been studied. The negative charge aids the retention of anionic PFAS and prevents fouling.[186] Ceramic membranes are traditional membranes that are widely used over polymeric membranes due to their high chemical and thermal stability, mechanical strength, and ability to overcome extreme environmental pH and temperature conditions. Microporous silica, glass, alumina, zirconia, and zeolites are used to fabricate membranes using chemical extraction, chemical vapor extraction, phase extraction, sol–gel process, and solid-state method. The major disadvantage of ceramic membranes is their lower efficiency in removing short-chain PFAS. Zhou et al.[187] manufactured a silica membrane functionalized with an octyl-perfluorinated chain and amino group. The F–F interaction between the silica surface and PFC perfluoroalkyl is enhanced by the electrostatic attraction of –NH$_2$ and –COOH with an adsorption capacity of 111.14 mg g^{-1}.[187] Graphene oxide (GO) functionalized with amine has been investigated for the rejection of PFOA from wastewater, which showed a removal efficiency of 74% with an initial concentration of 50 mg L^{-1}. The underlying principle of GO membranes is their ability to reject salt by changing their retention property, such as charge-based steric-based rejection, without affecting their low salt rejection properties, enabling the removal of PFOA.[161] Therefore, GO membranes are widely used for the treatment of industrial wastewater contaminated with PFOA. Metal–organic frameworks (MOFs) have been reported to be effective for the removal of PFAS using adsorption, owing to their large surface area and pore volume, high absorption capacity and conductivity, and structural diversity. A hydrophobic and hydrophilic double layer incorporated with MOF showed a rejection rate of 98.4% for PFAS.[162] MXene-polyamide-polysulfone + trimesoyl chloride nanocomposite membranes have also been used to enhance the PFOS rejection rate up to 96%. The main factors affecting the rejection rate are size and the interaction of PFOS with the membrane.[163] Similarly, NF270 membranes were used to obtain a rejection rate of 94.3% based on the size exclusion principle.[188] The use of MXene and tannic acid to develop an RO nanocomposite with 40% permeability and 11% antifouling against PFAS has been reported.[164] Phosphorene membranes were coupled with polyether ether ketone (PEEK) to obtain 99% elimination of PFOA.[165] However, the current membrane treatment technologies for PFAS still rely on traditional methods that cannot completely remove PFAS, producing a stream that must be securely destroyed. Therefore, PFAS destruction and separation should be addressed by future coupled technology. The adsorption of PFAS onto synthetically modified polymers, which are easily polymerized to have excellent affinity and specificity towards the target pollutants, has been studied in several experimental arrays. β-Cyclodextrin (β-CD), which is composed of urethane monomers, formed multilayer structures due to the adsorption of PFOA.[189,190] However, the polymer network was replaced by decafluorobiphenyl (DFB-CDP), which showed a higher removal effectiveness than CD and biochar.[191] Furthermore, a new adsorbent containing cross-linked chitosan for PFOS removal was developed using the molecular imprinting process, and its

adsorption rate was better than previously reported ones.[192] Table 3 reports the maximum adsorption capacities for various PFAS on different adsorbents.

5.1.2 Nano-filtration. Many per- and poly-fluoroalkyl substances (PFAS) of rising concern exhibit compound-specific nanofiltration (NF) efficiency, which can significantly impact the water matrix. The rejection of PFOS and PFOA in synthetic and industrial waters is enhanced by the presence of cations as complex formation between these chemicals and cations increases the rejection rate by NF (reference needed). An NF membrane demonstrated a PFAS elimination rate of 94.3% in water sources with various concentrations of humic elements, which is also influenced by colloidal particles.[188,215] Zhao et al. demonstrated the influence of cations (Ca^{2+}, Na$^+$, and Fe^{3+}) using a commercial NF membrane (ESNA1-K1); the rejection rate increased from 92.65% to 97.94% when the concentration of SO$_4$ and PO$_4$ increased to 2 mM.[166] Franke et al.[216] used NF270–400 membranes and achieved up to >98% a removal of PFAS and achieved additional water quality goals, such as the removal of uranium-238 and hardness.[216] Soriano et al.[217] reported a rejection efficiency of PFHxA as high as 99% using NF270 and NF90 membranes for 100 mg L^{-1} concentration.[217] Liu et al.[167] showed 97% removal rate for 42 different PFASs using nano-filtration NF270 membranes in a pilot membrane system setup. Steinle et al.[168] investigated the NF technique using four membranes (NF270, NF200, DK, and DL) against 15 PFAS, which showed rejection higher than 95% to anionic ions with a concentration of 300 g mol^{-1}.[168] Moreover, Boo et al. manufactured a membrane using a polyamide layer with a combination of bipiperidine and piperazine.[159] The NF membrane has a negative charge with a pore diameter of around 1.2 nm, which is substantially bigger than the commonly used commercial NF membrane (NF270). The membrane showed a high retention of 90% for PFOA in the presence of CaCl$_2$, NaCl, and Na$_2$SO$_4$.[159] Appleman et al.[218] coupled both NF and GAC methods to obtain a rejection rate >93%. The effect of DOM was demonstrated to cause >20% breakthrough of all the rejection rates.[218] Covalent organic frameworks (COFs) and MOFs have recently gained attention as potential fillers in advanced NF membrane technologies.[219] The inherent porous structure of MOFs can offer various molecular transport channels, which can reduce the water permeability and internal diffusion resistance, and hence increase the rate of removal in NF membranes. Additionally, MOFs and MOF-based membranes have demonstrated excellent properties for solid phase-extraction and high absorption capacity, which are suggested as potential candidates for the sorption of PFAS. MOFs with crystalline structures are highly specific, enabling the selective elimination of long- and short-chain PFASs.[220] For example, three metal nodes in the MOF series, MIL-53(Al), MIL-101(Cr), and MIL-53(Fe), have been prepared. Among them, MIL-53(Al) has the maximum PFOS adsorption capability due to the interaction of most of the unsaturated metal active sites with the smallest pore size of the membrane.[221] The addition of nanoparticles and adsorbent fillers to the polymeric membrane matrix appears to be a feasible strategy that has been shown to have a tremendous impact on the membrane performance for

Table 3 Remediation of PFAS by adsorption

Adsorbent type	Adsorption materials	Surface area (m^2 g^{-1})	PFAS initial conc. (ng L^{-1})	Adsorption capacity (mg g^{-1}) or removal (%)	Reference
Granulated activated carbon (GAC)	F400	769	350	—	193
	Carbsorb 40	755	350	—	
	Mesoporous carbon (HPC)	788	350	—	
	CMR400	767	350	—	
	Commercial GAC	815	1×10^8	178, 390	194
	F400 (untreated)	924	1×10^6	13.6, 12.3	195
	F400 (HCl-treated)	899		14.6, 13.4	
	F400 (NaOH-treated)	886		13.4, 12.2	
	F400 (H_2O_2/Fe-treated)	727		11.1, 9.4	
	F400 (persulfate-treated)	826		12.4, 11.6	
	CBC (untreated)	908		12.2, 10.8	
	CBC (HCl-treated)	886		13.0, 11.4	
	CBC (NaOH-treated)	897		11.3, 9.6	
	CBC (H_2O_2/Fe-treated)	706		9.2, 7.3	
	CBC (persulfate-treated)	870		11.1, 9.3	
	F400	784	1.51–431	0.015×10^{-3}-3.8×10^{-3}	196
Powder activated carbon (PAC)	PAC	1227	1×10^8	203, 535	194
	PAC	812	50×10^6	365.8	197
	CCAC AquaCarb	1126	500	Varying	198
	AWAC filtrasorb	929		(refer to the article heatmap)	
	Wood-based SPAC	927	1.51–431	0.015×10^{-3}-2630×10^{-3}	196
	Commercial PAC	953	500×10^6	1.9 mmol g^{-1}	199
ACF	PACFs	1781	1×10^8	302, 760	194
Amine-containing	Poly(N-[3-(dimethylamino)propyl] acrylamide, methyl chloride quaternary (DMAPAA-Q)	5.7	1000	90% removal	200
	poly(ethylenimine)-functionalized cellulose micro-crystals (PEI-fCMC)	7.8	1000	90% removal	201
	Covalent organic framework (28% [NH_2]−COFs)	1900	1000	90% removal	202
Amine-containing	Ionic fFluorogels (IFs)	—	1×10^3 or 50×10^3	80% removal	203
	DEXSORB	30	1000	75% removal	204
	DEXSORB+	19		62% removal	
	Amin-CDP	140		62% removal	
	Mg–Al LDHs	0.7	1×10^7	66% removal	205
MOFs	Zn–Al LDH	3.7	1×10^7	98% removal	205
	Zr-based MOF (NU-1000)	2255	1×10^7-1.1×10^8	201–622	206
	MIL-53(Al)	1336	5×10^6-1×10^8	66	207
	MIL-53(Fe)	1246		32	207
	MIL-101(Cr)	873		~10	
	NanoZIF-67	1660	5×10^8	734	208
	MacroZIF-8	1610	5×10^8	727	
	F-MOF	44	—	419	209
	MIL-96-RHPAM2	75	1×10^9	340	210
	MgCl$_2$-modified sugarcane biochar	81.3	10×10^3		211
Biochar	BMBC-600	79.87	70–4.8×10^5	90% removal	212
	BSBC-600	55.29	70–4.8×10^5	90% removal	212
	BS	111.78	3.93–23	236 μμmol /g^{-1}	213
	Sewage sludge biochar (SSBC1)	165	2.83×10^5-5.288×10^6	—	214
	Sewage sludge biochar (SSBC2)	87		—	214
	Wood chip biochar (WCBC)	683		—	

NF processes.[222] The applications of MOFs for the remediation of environmental pollutants have recently received great interest recently, which has the potential to completely transform NF technology by successfully capturing and removing PFAS from water.

5.1.3 Reverse osmosis. Reverse osmosis (RO) membranes are highly effective at eliminating many organic and inorganic

chemicals from water solutions. Recent advancements in manufacturing techniques, particularly those involving conjugated polymer chemistry, have significantly improved the selectivity of RO membranes for both short and long-chain PFAS. However, compared to other filtration methods, RO processes require high pressure, leading to increased energy costs. The operating pressures for RO systems range from 10 to

100 bar, depending on the feed osmotic pressure, to generate *trans*-membrane fluxes.[223] In the RO membrane matrix, the separation of molecules is based on their various diffusivities and solubility caused by the solution-diffusion process. The use of four thin-film RO membrane composites of polyamide (ESPA3 and LFC3) has been exploited for the removal of PFOS from photolithographic waste. The rejection rate is 99%, with a feed concentration of 1500 mg L^{-1} of PFOS.[169]

The integration of an RO membrane (TW30-1812-100) and UV/SO$_3$$^{2-}$ photo-catalytic system has been developed to reject PFOS from water. In comparison to the RO membrane, this system attained a PFOS rejection rate of 98.7% after 150 min. Further investigation revealed that the rate of degradation was inversely proportional to the initial PFOS concentration and correlated with the pH and the UV light intensity. The rejection is due to the electrostatic repulsion and membrane pore size, resulting in the adsorption of PFOS.[170] The degradation ability of PFAS at a water recycling facility in South East Queensland, Australia, using RO membrane technologies has been investigated. The most common PFAS found in the plant were PFOS PFHxS (20–40 ng L^{-1}), PFOA (14–29 ng L^{-1}), and PFHxA (38 ng L^{-1}). The recycling plant has a treatment that includes coagulation/flocculation, sedimentation, ultrafiltration (UF), RO, advanced oxidation, and final stabilization/disinfection. The PFAS levels were below the reported standards (0.4–1.5 ng L^{-1}) after RO treatment.[224] Baudequin *et al.*[171] studied the impact of fouling on various RO membranes, such as cellulose acetate (CD/CE) and polyamide composite (XLE and FT-30). The rejection rates achieved for the fluorinated surfactant (PFOA) in industrial and laboratory water samples was in the range of 99.4–99.9%, and the permeability was 0.5 L h^{-1} m^{-2} bar^{-1}. In this study, several membranes were evaluated. The fluorinated surfactant retention and flux drop were considered when choosing the best material, which was the composite PA membrane. The rejection rates for the fluorinated surfactant achieved at the industrial and laboratory scales for the composite membranes were in the range of 99.4–99.9%. During the initial absorption process, the membrane flux is reduced,

which can be due to the hydrophobic interactions; as the absorption process continues, the flux attains a steady state.[171] Size exclusion, electrostatic interactions, and hydrophobic interactions are crucial factors in the rejection of PFAS using reverse osmosis (RO) membranes. The overall performance of these membranes can be further enhanced by coupling various techniques or modifying the functionality of the membrane specifically for the PFAS removal process.[225]

5.2 Advanced oxidation processes

Advanced oxidation processes (AOPs) are methods using powerful oxidizing species (ROS) such as hydroxyl and sulphate radicals to snip C–F chains, remove the head groups, and break C–F bonds as shown in Fig. 8.[241] The various mechanisms for oxidation and reduction techniques include photocatalysis, persulfate activation, electron beam, UV/sulfite, ozonation, plasma, and sonochemical oxidation. The extensive use and environmental and health risks of PFCAs and PFSAs have prompted more research on their deformation by AOPs than other PFAS.[226,227] The characteristic properties and quantity of reactive oxygen species (ROS), along with operational variables such as the initial concentration of PFAS and pH, are significant factors influencing the breakdown of PFAS in oxidation processes.[228]

5.2.1 Persulfate activation. The mechanism begins with (decarboxylation) the removal of a carboxyl or sulphur trioxide group to liberate CO$_2$ or SO$_3$, substituting fluorine with hydrogen atoms (defluorination), and cleaving C–C bonds.[176,177] For instance, the decarboxylation of PFOA was achieved using an In$_2$O$_3$-activated persulfate system under solar light. In this process, the C$_7$F$_{15}$COO$^-$ radical is immobilized on In$_2$O$_3$ and oxidized by charge carriers (holes) to produce the C$_7$F$_{15}$ radical, a mechanism known as the "Kolbe decarboxylation process". Concurrently, sulfate radicals react with the generated alkyl radicals to form the C$_7$F$_{15}$OSO$_3$ radical. This process is proceeded by intra-molecular rearrangements such hydrolysis, HF elimination, and loss of a CF$_2$ unit. The gradual reduction of CF$_2$, and stepwise disintegration into shorter-
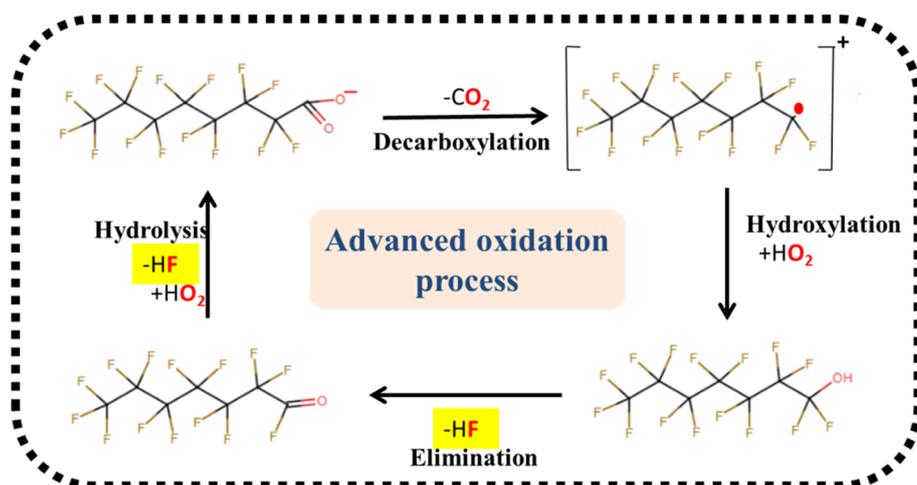

Fig. 8 Mechanism of advanced oxidation process.

chain PFCAs allows perfluorocarboxylic acids (PFCAs) in persulfate environments to degrade even further.[229] Sulfate radicals that are highly reactive break the C–S bonds in PFSAs by removing their electrons to produce unstable alkyl radicals. Then, deformation occurs similar to hydroxyl radicals, i.e., hydrolysis and loss of hydrogen and fluorine ions.[230] The various persulfate activation methods (degradation%) reported are Al_2O_3 + PA (100%),[231] PMS/Ga_2O_3/UV (100%),[232] solar light/In_2O_3/PA (98.6%),[3] heat/zeolite/PS (99.8%),[2] UV/ZnO/ozonation/PS (100%),[178] and heat/PS (97%).[1]

5.2.2 Photo-catalytic oxidation. Electrons, holes, hydroxyls, and superoxide radicals play a vital role in photo-catalytic oxidation. During illumination, the semiconductor/material conduction and valence bands produce electrons and holes, respectively. The holes and water molecules form hydroxyl radicals; electrons and oxygen produce superoxide radicals.[233] Different pathways have been explained in the literature to characterize the PFAS products in photo-catalytic degradation. For example, $Zn_xCu_{1−x}Fe_2O_4$ has been used with oxalic acid to generate reactive species that showed 87% degradation of PFOA by the decarboxylation of an electron in a reaction time of 120 min.[179] BiOF nanosheets were used to oxidize PFOA by H^+ and O_2 radicals to produce unstable perfluoroalkyl ($C_7F_{15}COO^−$), which proceeded by interacting with H_2O/O_2. Then HF is lost to generate $C_6F_{13}COF$, which is then hydrolyzed to form $C_6F_{13}COOH$ (PFHpA). The final degradation of the short-chain PFCAs into F and CO_2 was achieved by progressively removing the CF_2 units and achieving 100% degradation in 360 min.[180] $Pt/La_2Ti_2O_7$, along with methanol, was used for the photocatalysis of PFOA, which degraded about 50% in 1440 min.[234] Ga/TNTs with AC were used as an absorbent and a treatment technique for PFOS; the degradability attained was 75% in 240 min.[235]

5.2.3 UV/sulfite. In this process, sulfur trioxide radicals and unbound electrons are released when sulfite solutions are exposed to UV radiation. The first transformation of PFOA into $C_7F_{14}SO_3H–COO^−$ shows that a fluoride ion was replaced by a sulphur trioxide group via a reaction with a sulphur trioxide anion radical or water, and intermediate products were generated.[236,237] Liu et al.[181] demonstrated that a combination of UV with NF would be an effective technique by treating 12 PFAS/PFCA, which showed 95% rejection in 120 min.[181] According to a study conducted by Tenorio et al.,[236] UV/sulfite systems are more reactive to PFCAs than PFSAs of similar chain length, i.e., PFOA are 5 times more reactive than PFOS.

5.2.4 Electron beam. When water samples containing PFAS are subjected to a beam of electrons, the water absorbs the energy and generates a variety of radical intermediates, including H^+ and O_2 radicals. These radicals break down the long chain into a shorter chain.[13] According to Yamijala et al.,[182] the formation of alkene bonds (C=C) rather than alkane (C–C) is accompanied by losing fluorine atoms, which starts the disintegration of PFAS by extra electrons. This is consistent with the results reported by Trojanowicz et al.,[183] who reported that acetate and formate as by-products of PFOA breakdown produce carbon dioxide radical anion (CO_2) during the electron beam and gamma irradiation procedures.

Similar to other techniques, the plasma process generates oxidizing intermediates such as hydroxyl and carboxyl radicals. This technique is accompanied with UV irradiation, thermal and electric methods to enhance the photo-catalysis of C–C bonds. According to Singh et al., the decomposition of PFSO and PFOA into PFPeA, PFHpA, PFHxA, and PFBA suggests the sequential removal of CF_2 to form shorter-chain PFCAs without the breaking of the carboxylic head group with a removal rate of PFOA up to 77%.[238] The cavitation mechanism, which causes shock waves at extremely high-temperature levels around bubble interfaces, causes the rise and bursting of micro-bubbles. This sonochemical technique is used to degrade PFAS by about 97% at 400 Hz. This study also demonstrated that there was no PFAS degradation at high frequencies (1000 Hz).[239] Ozone acts directly on unsaturated bonds to break down complex substances. However, it typically has excellent capacity for degradation when it is aided by UV light, which generates H_2O_2, followed by hydroxyl radicals.[240] However, the main challenges in the application and commercialization of e-beam technology for the removal of PFAS from water are the initial costs, high energy demand and complexity of the treatment.

5.3 Adsorption onto activated carbon

One of the most prevalent adsorbents used in the treatment of wastewater and water is AC. The adsorption technique using AC is influenced by various variables, including surface area, surface chemistry, pore size distribution (PSD), polarity, functional groups, solubility of the absorbent, and working conditions of the PFAS solution. Agriculture-based raw materials, such as agro-waste, have been widely employed as an alternative to commercial AC for the removal of organic containments from water systems. The poor hydrophobicity of AC can remove short-chain PFAS compared to long-chain PFAS.[242] Nevertheless, there is a lack of research on its application for PFAS elimination. There are several commercially available adsorbents for the removal of PFAS, such as GAC: Filtrasorb 400, multi-walled carbon nanotubes (MCN), powdered activated carbon, double-walled carbon nanotubes, anion-exchange resin AER: IRA67, silica, and alumina. A high PFOS/PFOA removal efficiency was found in MCN, AER, and GAC (98%), which was attained in 24 h after absorption equilibrium.[243] The treatment of PFAS-containing water has been achieved using biochar, a class of natural material-based adsorbents. The waste biomass is pyrolyzed in a low-oxygen atmosphere, which produces a low-cost carbon residue, biochar.[172] Zhang et al. used both GAC and biochar (softwood-derived) owing to their ability to bind to PFASs, including PFOA, PFBA, PFOS, and PFBS. The biochar required 12–48 h to achieve equilibrium, whereas PFAS adsorption on GAC reached equilibrium within about 3–24 h. Electrostatic attraction and hydrophobic contact were explained as the major mechanisms in the sorption process, which has a great influence on the change in pH, i.e., as the pH dropped, there was an upsurge in PFAS sorption.[173] It was found that quaternary ammonium/epoxide with activated carbon (QAE-AC) considerably improved the adsorption of PFOA from water. Changing the QAE/AC ratio resulted in morphological variations in AC.
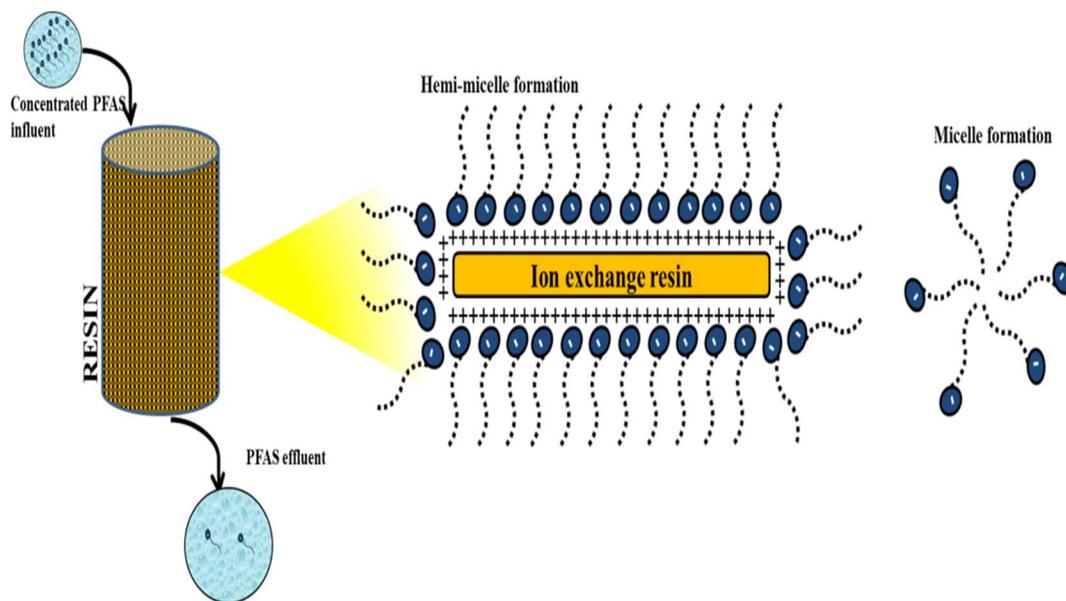
Fig. 9 Mechanism of anion exchange process.

PFAS was able to enter the internal pores of AC at a moderate concentration of QAE and produce hydroxyl radicals and carboxyl radicals on the graphene sheets of the AC matrix.[244] To effectively utilize these materials, it is crucial to manage the life cycle of the adsorbents and their regeneration capabilities in a cost-effective manner. Unfortunately, well-defined strategies and methods for achieving this have not been fully established to date.

5.4 Ion exchange process

The process of reversibly transferring negative ions, such as OH^-, Cl^-, and HCO_3^-, from the polymeric resin surface to its surrounding aqueous matrix is known as anion exchange (Fig. 9).[245] The ion exchange (IE) technique using anion exchange resins is a realistic solution that demonstrates great potential for the efficient removal of PFAS from water. Resins are divided into two types, *i.e.*, type I, trimethyl ammonium group, and type II, dimethylethanol ammonium group, based on their functional groups, degree of cross-linking, and the polymeric matrix. Based on their level of resistance to pH range, resins are categorized into weak-base IX resins and strong-base IX resins.[246] The commercially available resins for PFAS removal are Amberlite™ PSR2 Plus, Purolite A592E, GenX, Resin Tech SIR-110-HP, and Purolite A694E with an exchange capacity of 0.7, 09, 0.8, and 1.2 eq L^{-1}, respectively.[174] The diffusion mechanism in an IE system during PFAS removal is described using the intra-particle diffusion model.

The adsorption of PFAS is impacted by pore diffusion in the presence of inorganic ions and pH. A solute–solute interaction is formed between PFAS, such as the generation of monolayer hemimicelles, bilayer admicelles, and micelles, which causes molecular aggregation. Positively charged resins can absorb PFAS more effectively when multilayer structures such as admicelles and hemimicelles are formed.[247] Gagliano *et al.*[175]

showed a recovery of 90% for PFOA using a Macronet resin. Dixit *et al.*[248] compared the performance of a conventional A860 resin with A592 special resin for PFAS, which showed a removal efficiency of 95%. However, PFAS-specific resins used in industrial applications need to be explored for their mechanism, whether the absorption process is chemisorption, hydrophobic interactions, or electrostatic interactions.[249] Table 4 lists the recovery rates as well as the regeneration conditions of different resins toward various PFAS.

5.5 Biological process

The chemical structure of PFAS is the most crucial characteristic for their biodegradation. A wide range of functional groups, including carboxylates (–COO^-), amines, sulphates (–SO_3^-), sulfonates, and phosphates (OPO_3^-), play a remarkable role in the degradation process and control the thermal-chemical stability of PFAS and their precursors in the environment. The nature of the transformations of PFAS molecules and their and quantity depend on their structure, which affects defluorination and biotransformation reactions. The co-substrates, growth stimulants, and organic content play a significant role in biotransformation. 1-Butanol, *N*-octane, and lactate are common substrates that have both positive and negative effects on biotransformation. Short-chain fluorinated carboxylic acids were studied for their structure-specific biotransformation under aerobic conditions, and it was shown that only C–F bonds and C–H were susceptible to microbial breakage. The studies also showed that C–F bonds were essential for microbial defluorination through oxidation-type pathways.[262] Unsaturation is essential for the biotransformation of PFCA through reductive defluorination and/or hydrogenation pathways, as demonstrated by Yu *et al.*,[263] where two C6 branched and unsaturated fluorinated carboxylic acids (FCAs) were selected. C–F bonds were replaced by C–H

Table 4 Remediation of PFAS by ion exchange resins

Ionic exchange resin	PFAS used	pH	Regeneration conditions	Recovery rates	Reference
IFs	GenX	6.4	Ammonium acetate (400 mM) in 50% aqueous ethanol (20 mL)	75%	250
IRA 67	PFOS	3	70% methanol + 1% NaCl or 1% NaCl/ methanol (10 g: 30 mL resin to regenerate ratio, magnetic stirrer at 170 rpm for 12 h at 25 °C)	98.9%	251
		4		99%	252
	PFOS	3	1% NaOH + 70% methanol, 150 rpm, 24 h at T = 25 °C	98.7%	253
IRA 458	PFOS	—	320 mM NaOH (ratio unspecified, resin in packed glass column (1 cm diameter and height 10 cm), operated at 20 mL min^{-1} for 12 h at 20 °C)	0.3%	254
IRA 958	PFOS	3	Methanol (10–70%) + 1% NaCl (20 mg: 100 mL resin to regenerate ratio, orbital shaker at 150 rpm for 24 h at 50 °C)	4.2–90.8%	251
DOW V493	PFOS	6.4	Methanol (LC-MS Grade)	100%	255
A600E	PFOA	3	3% NH$_4$Cl + 3% NH$_4$OH (1 g: 1 L resin to regenerate ratio, flash stirred for 60 h at 20 °C)	85%	256
	PFOA, PFOS PFBA, PFBS	—	0.5% Ammonium chloride (NH$_4$Cl) + 0.5% Ammonium hydroxide (NH$_4$OH)	63% (PFOA), 48% (PFOS), 68% (PFBA) and 41% (PFBS)	257
	PFOA, PFOS PFBA, PFBS	7.5	(5 g: 250 mL resin to regenerate ratio, magnetic stirrer at 250 rpm for 80 h at 20 °C)	51% (PFOA), 39% (PFBA) 55% (PFOS) and 48% (PFBS)	258
	PFOA	7.5	2% NH$_4$Cl and 1% NaCl (5 g resin: 250 mL regeneration solution), 250 rpm at 20 °C in a thermostatic oven for 80 h	—	259
A520E	PFOA, PFOS PFBA, PFBS	3, 7.5	0.5% NH$_4$Cl + 0.5% NH$_4$OH (5 g: 250 mL resin to regenerate ratio, magnetic stirrer at 250 rpm for 80 h at 20 °C)	90% (PFOA), 74% (PFOS), 84% (PFBA) and 82% (PFBS)	256, 259 and 258
A532E	PFOS	3	80% Alcohols (methanol/ethanol (C$_2$H$_5$OH) + 1% NH$_4$Cl (1 g: 1 L resin to regenerate ratio, flash stirred for 60 h at T 20 °C)	90%	256 and 258
A860	PFOA, PFOS, PFBA, PFBS and GenX	7	10% NaCl (10 bed volumes (BV) (*i.e.*, 1 mL resin with 10 mL brine for 1 h at 21 °C)	95%	260
Purosorb PAD 500	PFOA	3, 7.5	30% Methanol (5 g: 250 mL resin to regenerate ratio, magnetic stirrer at 250 RPM for 80 h at 20 °C)	20%	256 and 259
Macronet MN102	PFOA	3, 7.5	50% Methanol + 3% NH$_4$OH (5 g: 250 mL resin to regenerate ratio, magnetic stirrer at 250 RPM for 80 h at 20 °C)	90%	256 and 259
Sorbix A3F	PFOS	—	Organic solvent + brine	—	261

bonds due to hydrogenation. Various sources, including landfills, contaminated soils WWTP effluents, sludge, lakes, and sea sediments (aerobic, anaerobic, and anoxic), have evolved bacterial species with the capacity to transform/degrade and/or defluorinate PFAS. Yang *et al.*[264] selected *Rhodococcus jostii* RHA1 bacterium to defluorinate 6 : 2 FTSA. The two major enzymes responsible for deformation are cytochrome P450 and alkane monooxygenase, which were highly expressed in 6 : 2 FTSA cultures. These defluorinating and desulfonating enzyme genes serve as possible indicators to measure the biotransformation of 6 : 2 FTSA. *Pseudomonas* spp shows resistance to fluoride, and some of their strains can catalyze the defluorination of PFAS. The mechanism of sensing and degrading fluoride in the cells is through the Fluc/FEX/CLCF family F channels or

F/H+ antiporters.[265] The biotransformation of PFAS has been associated with several bacterial species, including *Pseudomonas butanovora*, *Mycobacterium vaccae*, and *Pseudomonas oleovorans* for 6 : 2 fluorotelomer alcohol,[184] *P butanovora + P. fluorescens* for FTOHs,[266] Acidimicrobiaceae sp. strain A6 for PFOA,[9] *Acidimicrobium* sp. strain A6 for PFOA-PFAS,[8] *Gordonia* sp. for 6 : 2 fluorotelomer sulfonamidoalkyl betaine,[267] *Pseudomonas parafulva* for PFOA,[268] *Pseudomonas aeruginosa* for PFOS,[269] *Pseudomonas plecoglossicida* for PFOS,[270] and *Dietzia aurantiaca* for 6 : 2 FTS.[4] The majority of PFAS compounds are converted into terminal perfluorinated carboxylic acids. Isolating microorganisms that can break down long-chain chemical structures and promote biodegradability is a significant challenge in current research. The resilient

microorganisms that can degrade PFAS at the appropriate rates and extent with proactive efforts are more promising in resolving PFAS. Before bioremediation may be used as an effective industrial method for the degradation of PFAS, there is a plethora of obstacles and problems that still needs to be addressed. Table 5 report previous studies on the bioremediation of PFAS including the involved microorganisms and the optimum conditions for the removal process.

5.6 Hydrothermal liquefaction (HTL)

Hydrothermal liquefaction (HTL) is a traditional strategy for recovering the energy from wastewater sludge, which generates liquid bio-crude oil by subjecting aqueous slurry-based sludge to temperatures and pressures in the range of 250 °C to 350 °C and 10 to 25 MPa, respectively, which are higher than the water vapour pressure to prevent water vaporization.[285] HTL avoids the high energy needs associated with water vaporization; thus, it is the best approach for treating wet organic solids such as sludge. Additionally, liquid fuel by-products have an economic advantage compared to biogas generated by anaerobic digestion.[286] >99% PFOA, 7 : 3 FTCA, and 8 : 2 FTUCA were converted at 350 °C for 90 min. Nevertheless, a more constrained transition was shown for sulfonic acid structures, with 34% PFOS degradation and 67% 8 : 2 FTS degradation. Therefore, the findings imply the partial mineralization of PFAS.[151] According to Wu *et al.*,[287] HTL could eliminate PFOS in a solution when it has been altered with NaOH. Similarly, Hori *et al.*[288] showed that HTL could efficiently degrade PFOS and other perfluorosulfonic acids (PFSAs) containing shorter carbon chains when zero-valent iron is present in the medium. The sorbed pollutants and other organic compounds in the sludge will be degraded and mineralized under HTL conditions, but there is a chance that extremely resistant substances such as PFAS might remobilize into the by-product aqueous phase. Therefore, it is critical to determine the lifecycle of PFAS during the HTL process.[289] However, the HTL technique is efficiently adaptable to break down the PFAS accumulated in plant biomass/wet sludge.

5.7 Others

It has been shown that aquatic plants can quickly decrease the amount of PFAS in heavily polluted lake water. For example, seventeen surface and one submerged species of wetland plants were evaluated for PFAS absorption. *Elodea canadensis*, *Carex rostrata*, and *Eriophorum angustifolium* had the highest amounts of PFAS. Following that, these species were employed for enzyme research as well as an investigation into the impact of biomass on the removal of PFAS from water. The findings demonstrated that the PFAS removal effect increased with biomass content per volume. Although their degradation also occurs, plant absorption is primarily responsible for the plant-based removal of PFAS from water.[290]

The main place to dispose of material containing PFAS is landfills, where landfill leachate releases PFAS into the surrounding environment. Owing to its elimination of over 90% long-chain PFAS, ozone foam fractionation shows promise as a PFAS removal method. In industrial applications, the determined operating parameters offer insightful guidance for optimizing the ozone flow rate (1 L min^{-1}), dosing (43 mg L^{-1}), and reducing foamate generation (4% wettability). According to equilibrium modeling, for a given PFAS concentration, the excess surface of air bubbles is 20–40% more than that of ozone bubbles. Notably, ozone foam fractionation produces foamate quantities that are two to four times lower, which lowers the need for site storage and saves a lot of money in waste product disposal.[291]

For the first time, three distinct hydrodynamic cavitation reactor set-ups, each improved with surface alterations incorporating roughness elements, were used to test the hydrodynamic cavitation on a chip concept (HCOC) for the degradation of 11 prevalent PFAS variations. Three different microscale hydrodynamic cavitation (HC) reactors were used to completely establish cavitating flow treatment for Stockholm municipal wastewater treated by Membrane BioReactor (MBR) technology. The results show that almost all the PFAS compounds can be broken down by the chemical-free HCOC technique at a noteworthy rate of 36.1%. When combined with the MBR process, this technique can also prevent blockages in the fluidic channels, allowing continuous operation at high throughput processing rates.[292]

In conclusion, it is important to note that among the adsorbents, activated carbon and ion exchange resins have been predominantly employed due to their proven effectiveness, particularly in column and batch modes. These materials are highly effective for long-chain PFAS removal because of their greater hydrophobicity and the formation of hemimicelles or micelles on the adsorbent surface. However, they exhibit slow adsorption kinetics and lower affinity for short-chain PFAS, limiting their overall efficiency. Amine-containing adsorbents show promising potential with faster adsorption kinetics and higher adsorption capacities than traditional adsorbents, but they require further research for full-scale applications. Additionally, new-generation adsorbents such as molecularly imprinted polymers (MIPs) and nanoparticles have been explored for selective PFAS removal and detection in water, but the disposal of these adsorbents poses significant challenges. The effectiveness of membrane technologies for PFAS removal varies significantly. Low-pressure membranes, including microfiltration (MF) and ultrafiltration (UF), are generally ineffective for PFAS removal. Conversely, reverse osmosis (RO) and nanofiltration (NF) membranes are highly efficient, though they are energy-intensive and produce large volumes of PFAS-concentrated waste, necessitating further treatment before disposal. Functionalized membranes offer promising potential for PFAS removal but face significant challenges related to scalability and practical application. Earlier studies on PFAS removal often focused on a limited number of target PFAS in synthetic water at concentrations higher than that typically found in real water samples. Experiments conducted in real groundwater have revealed that background ions and compounds can inhibit the removal of PFAS, highlighting the need to mitigate these effects in real contaminated water. This remains an open field of research, emphasizing the need for continued exploration and development of effective PFAS removal strategies.

Table 5 Bioremediation of PFAS

Microorganism/Plant	Growth conditions	Initial concentration	Removal rate	Transformed products	Reference
Acidimicrobium sp. strain A6	Anoxic inorganic Fe(III)–NH$_4^+$ enrichment medium	100 mg L^{-1}	60%	PFHpA	271
Pseudomonas plecoglossicida 2.4-D	26–30 °C, pH 6.8–7.2, 0–5% NaCl aq	1.0 g L^{-1}	75%	PFHpA	272
Pseudomonas parafulva	30 °C, pH 7, 2% inoculum	500 mg L^{-1}	32.4%	—	268
Pseudomonas aeruginosa strain HJ4	C Medium and Luria Bertani, pH 7	600 mg L^{-1}	67%	—	273
Zymogenous	Nutrient Agar, 28 °C	1 µg mL^{-1}	46–69%	Monofluorinated fatty acid	274
Cannabis sativa L.	pH 6.28	~760 µg L^{-1}	98%	Perfluoro carboxylic acids & perfluoroalkyl sulfonic acids	275
Gordonia sp. NB4-1Y	Sulfur-limited conditions	83.1 mol%	99.9%	6 : 2 FTCA, 6 : 2 FTUA, and 5 : 2 fluorotelomer ketone	276
Rhodococcus jostii RHA1	Ethanol-rich medium	168 mg L^{-1}	—	6 : 2 FTUCA and 5 : 3 FTCA	277
Acidimicrobiaceae sp. strain A6	Anaerobic, pH 6.5–7.5	47.1 mg L^{-1}	77%	PFBA, PFPeA, PFHxA, PFHpA and F−	278
WWTP activated sludge	Aerobic, RT	1.4–1.5 mg L^{-1}	—	PFPeA, PFBA	279
Pseudomonas oleovorans, P. fluorescens DSM 8341	Aerobic, pH 7, 30 °C	2 mg L^{-1}	—	PFPeA	280
KB1 enrichment culture dominated by *Dehalococcoides*	Anaerobic, 34 °C	20.7 mg L^{-1}	>90%	FTMeUPA	281
Consortium	Aerobic, pH 7	0.75 mg L^{-1}	85%	8 : 2 FTCA, 8 : 2 FTUCA, PFOA	282
Soil microorganism	Aerobic	4.22 nmol g^{-1}	—	FTOHs, 6 : 2 diPAP → 5 : 3 acid, PFPeA, PFHxA, diPAP → PFOA	283
WWTP-activated sludge	Aerobic	1 mg L^{-1}	—	FTOHs and its degradation PFCA metabolites	284

6. Factors affecting PFAS removal

This section aims to explain the various variables that affect the removal of PFAS, such as pH, chain length of PFAS, dissolved oxygen matter, PFAS initial concentration, solubility, phase, and volatility of PFAS.

6.1 pH

One of the leading causes of PFAS adsorption/membrane separation inhibition in groundwater is pH. High pH levels inhibit anionic PFAS from adhering to substrates by deprotonating their functional groups. Depending on the isoelectric point of the PFAS and moieties at the surface of the membrane, alterations in the pH of the solvent may have an impact on the surface charge of the membrane.[293] Additionally, in some cases, altering the pH might affect the pore size, charge, permeability, and rejection rate of the membrane,[294] *i.e.*, the positively charged membrane surface traps negatively charged anionic PFAS, lowering the rejection rate. Alternatively, electrostatic interaction between anionic PFAS and non-polar membranes can improve the efficiency of PFAS removal.[295] According to Niu *et al.*,[296] the deprotonation of a fabricated membrane resulted in an excellent rejection rate at acidic pH. The used substrates were PAN-CGF and PDA-CGF, which were positively charged upon the protonation of PAN and PDA at pH 3.9 and 3.4, respectively, in a PFOA eradication investigation utilizing CGF-functionalized polymers in the pH range of 3–10. With an increase in pH, the PDA-CGF or PAN-CGF adsorption

capabilities declined steadily over time, which was attributed to the diminished electrostatic affinity between CGFs and PFOA. The removal capacities of PFOA and PFOS from rGO-ZF@CB declined significantly with an increase in the solution pH, indicating that the protonated functional groups of rGOZF@CB successfully adsorbed anionic PFOS and PFOA through electrostatic forces. The sorption capacity for both compounds was attained at pH 3, where protonation of rGOZF@CB was possible only in an acidic environment.[297] This suggest that acidic conditions are favourble for the removal of PFAS in general.

6.2 Ionic concentration

The interaction of various ions with PFAS present in water plays an essential role in their removal. Ionic strength often has a low impact on PFAS-contaminated water treatment. However, more attention must be given to extremely contaminated water sources, including industrial effluent, which has a high PFAS content and ion concentration. Ions in the water can attach to PFAS and develop complexes that may potentially result in temporary porous blocking in the membrane and block the absorption binding sites in due to the electrostatic attraction between the ions and PFAS present in the water. This mechanism lowers the removal of PFAS by decreasing the fate of long- and short-chained PFAS through the membrane. Additionally, an increase in the number of valence ions in the water can enhance the electrostatic interaction between ions and PFAS, promoting the aggregation of PFAS. Different amounts of MgCl$_2$, NaCl, or FeCl$_3$ were used as the baseline electrolyte to

assess the effect of cations on the sorption of PFOA by functionalized CGF polymers. With an increase in the cation concentration, the PFOA adsorption capabilities steadily increased. This was attributed to the increment in positive charges on the polymer substrate, which causes intermolecular attraction between the substrate and PFOA and intra-molecular repulsion between the PFOA molecules and the multi-ion salt bridges between the polymers and PFOA.[298]

The concentration of PFOS and PFOA sorption increased with increasing the concentration of NaCl by kaolinite.[299] Perfluoroheptanoate (PFHpA) and perfluorohexanesulfonate (PFHxS) in wastewater sludge were studied for the impact of cations on the partition characteristics.[300] The solution chemistry of PFOS sorption (pH, Na$^+$, and Ca^{2+}) was shown on the surface of mineral absorbents (silica and goethite), proving that the cations had different impacts on these two absorbents.[301] The concentration of the three main cations was varied (Na$^+$, Ca^{2+}, and Mg^{2+}) *via* the sorption coefficient (K_d) to check the absorption of 18 anionic PFAS in soil, and it was suggested that a higher cation content can result in lower PFAS mobility and removal. This suggests that ionic strength has different impacts on the removal of PFAS.

6.3   Chain length of PFAS

PFAS are omnipresent due to their oleophobic and hydrophobic properties. The chain length of PFAS (C_nF_{2n+1}) has a significant impact on both their characteristics and removal. The toxicity of PFAS increases with their chain length. Long-chain PFAS have a longer hydrophobic "tail," and thus they are anticipated to be more hydrophobic compared to short-chain PFAS. According to reports, short-chain PFAS are mobile and persistent in long-distance transport compared to their long-chain homologs.[302] In the membrane filtration technique for water and wastewater containing PFAS, long PFAS are susceptible to reacting with solid porous surfaces. Therefore, by combining filtration and adsorption, hydrophobic membranes may be useful in the removal or ejection of long PFAS.[303,304] Short-chain PFAS have shown comparable persistence to their long-chain homologs and are more mobile during long-distance transport. In water samples collected from Dagu Drainage Canal (Dagu) in Tianjin, China, short-chain PFAS were found to be comparable to longer-chain PFASs (>C6), and perfluorobutyric acid (PFBA) was the predominant short-chain analogue.[305]

6.4   Dissolved oxygen matter

Dissolved oxygen matter (DOM) is hydrophobic in nature; it has two conflicting effects on PFAS adsorption, where it competes against PFAS for the adsorption sites and provides PFAS adsorption sites based on the level of DOM in the water. Various organic substances, including hydrophilic acids, amino acids, phenolic groups, proteins, and Fe/Al oxides, are present in water, which create electrostatic attraction due to their cations along with DOM to form a complex with PFAS.[175] In the presence of sodium alginate and bovine serum albumin, the removal rates for PFAS were examined; the findings showed that both had the potential to increase the rejection rate of PFOS and PFBS.[306]

6.5   PFAS concentration

The removal efficiency of PFAS depends on their initial concentration in the water sample. Various studies have been performed with a high concentration of PFAS (100 ppm), and it was found that the removal efficiency is comparatively low.[307] The reason for the low removal is that when concentrations approach the threshold micelle concentration, a high PFAS content in the sample can cause micelle growth. The threshold micelle concentration can be achieved in groundwater and wastewater, but in the case of industrial wastewater, micelle growth increases and prohibits PFAS removal using different techniques, such as absorption and membrane filtration.[11]

6.6   Solubility of PFAS

The worldwide sources for PFAS are groundwater and surface water because of their high-water solubility. Therefore, drinking water sources are influenced by the presence of PFAS. The solubility of PFAs is compared to that of benzene. It is observed that PFOS has a 2.6-fold lower water solubility than PFOA, and 5.3-fold greater water solubility than benzene.[308] Neutral PFAS such as FTOHs and FOSEs are usually more volatile and found in the atmosphere, while ionic PFAS such as PFCAs and PFSAs are soluble and tend to be present in water/wastewater.[309] *N*-PFAS can be converted to i-PFASs, such as PFOA, primarily by biological and photochemical processes.[10]

6.7   Volatility of PFAS

Weak van der Waals (vdW) interaction is a characteristic that defines PFAS; thus, they tend to diffuse into the environment until they form a stable complex with a significantly specific interaction such as between i-PFAS and water. PFAS develop fragile intermolecular connections with their surrounding phase. It is estimated that the hexadecane/air partition coefficient (KH$_{xd}$/air) provides a qualitative approach to determine the vdW interaction in neutral solutes.[310] The partition coefficients of *n*-PFAS are forecasted using different phase partitioning methods to calculate KH$_{xd}$/air, which is a reliable indicator of their volatility, octanol/air partition coefficient, and saturated vapor pressure.[311,312] Hammer *et al.*[310] calculated the KH$_{xd}$/air values for 64 PFAS using modeling software such as an iterative fragment selection quantitative structure–property relationship (IFS-QSPR) model and a quantum chemistry-based prediction model (COSMOtherm). These simulations underrated the partition coefficient of PFAS based on the length of the perfluorinated alkyl structure, *i.e.*, short-chain PFAS are more volatile and can easily diffuse in the surrounding environment, making them difficult to remove.[313] The atmospheric transmission of PFAS volatile compounds is also shown by their existence in desolate areas, such as the Arctic, where the concentration has reached 26 pg m^{-3} for 8 : 2 FTOH.[314]

6.8   Phase of PFAS

One of the most crucial mechanisms to regulate the removal of PFAS is based on the partitioning between the mobile and stationary phases. Air and water are the mobile phases. Stationary

Table 6 Suitable methods for the removal of PFAS based on their properties

Removal method	Effectiveness	Suitable for long-chain PFAS	Suitable for short-chain PFAS	Energy consumption	Waste generation	Scalability	Challenges
Activated carbon	High for long-chain PFAS	Yes	Low	Moderate	Moderate	High	Slow kinetics, low affinity for short-chain PFAS
Ion exchange resins	High for long-chain PFAS	Yes	Low	Moderate	Moderate	High	Slow kinetics, low affinity for short-chain PFAS
Amine-based adsorbents	Potentially high	Yes	Yes	Moderate	Moderate	Medium	Requires further study for full-scale application
Molecularly imprinted polymers (MIPs)	Selective removal	Yes	Yes	Low to Moderate	Disposal issues	Low to Medium	Disposal challenges, practical implementation
Microfiltration (MF)	Low	No	No	Low	Low	High	Ineffective for PFAS removal
RO	High	Yes	Yes	High	High (concentrated waste)	Medium	Energy-intensive, waste management
NF	High	Yes	Yes	High	High (concentrated waste)	Medium	Energy-intensive, waste management

phases are soils, NAPLs, stream sediments, aquifer materials, and interfaces between phases (air–water, NAPL-water).[315] Geochemical variables, such as pH and temperature, can have major effects on partitioning given that PFAS are charged in electrostatic processes.[316] The quantity of PFAS stored in each system increases when a mass fraction of the PFAS is divided into immobile phases, which lowers the rate of their movement in the mobile phase.[317] Based on the properties of PFAS, their suitable removal methods are summarised in Table 6.

7. Conclusions and future perspectives

This study underscores the critical and growing concern surrounding per- and polyfluoroalkyl substances (PFAS) as persistent environmental micropollutants. Due to their strong C–F bonds, PFAS exhibit exceptional thermal and chemical stability, bioaccumulate through trophic levels, and persist in various environmental compartments, including the soil, water, air, and biota. Their documented toxicological effects on humans, plants, and animals, ranging from endocrine disruption and immunotoxicity to developmental and reproductive impacts, highlight the urgent need for their robust monitoring and mitigation strategies. The analytical detection and quantification of PFAS have advanced significantly, with methods such as solid-phase extraction (SPE) coupled with liquid chromatography–tandem mass spectrometry (LC-MS/MS) offering high sensitivity and selectivity. However, challenges remain in achieving ultra-trace detection limits, minimizing matrix interferences, and differentiating among thousands of structurally diverse PFAS compounds and their transformation products.

Regarding remediation, promising technologies, such as adsorption, membrane separation, ion exchange, and advanced oxidation/reduction processes (AOPs/ARPs), demonstrate potential for the effective removal of PFAS. Nevertheless, issues such as high energy consumption, incomplete mineralization, generation of toxic intermediates, and limited applicability to short-chain PFAS continue to hinder their large-scale implementation.

Bioremediation and phytoremediation represent emerging eco-friendly alternatives, though the metabolic pathways and microbial enzymes responsible for PFAS degradation remain poorly understood. Developing genetically engineered microorganisms or enzyme systems capable of cleaving C–F bonds could significantly advance this field. Further, the chain-length-dependent adsorption behavior of PFAS complicates the treatment optimization. Short-chain PFAS exhibit higher mobility and lower adsorption affinity, necessitating specialized sorbent designs and tailored operating conditions. Environmental parameters including pH, ionic strength, co-existing organic matter, and redox potential further modulate the removal efficiencies, emphasizing the need for comprehensive mechanistic studies.

Future research should prioritize the development of sustainable, bio-based adsorbents with high selectivity and regeneration capacity, and the integration of hybrid treatment systems combining physical, chemical, and biological processes for enhanced PFAS removal. Comprehensive life cycle assessments (LCAs) are needed to evaluate the environmental footprint of remediation technologies, while studies on the transformation and fate of PFAS precursors will aid in accurately assessing the total fluorine content and associated risks. Advancing real-time, on-site monitoring techniques and evaluating the scalability and cost-effectiveness of emerging treatment approaches for full-scale wastewater and drinking water applications are equally important. Ultimately, mitigating PFAS contamination requires a multidisciplinary framework integrating analytical chemistry, materials science, environmental engineering, and toxicology. Strengthening the mechanistic understanding and fostering innovation in detection and treatment technologies will be critical for minimizing PFAS exposure, protecting ecosystems and human health, and advancing environmental sustainability.

Author contributions

Pavithra N, Simranjeet Singh, and Radhika Varshney contributed equally to this work, including to the experimental design, data collection, and preparation of the original draft. Vishakha Chauhan was responsible for preparing and organizing the tables.

Retinder Kour contributed to writing, review, and editing of the manuscript. Nabila Shehata assisted in the review, writing and manuscript refinement. Praveen C. Ramamurthy supervised the overall study, provided conceptualization and guidance, and contributed to the critical review and final editing of the manuscript.

Conflicts of interest

There are no conflicts to declare.

Data availability

No primary research results, software or code have been included, and no new data were generated or analysed as part of this review.

Acknowledgements

References

1 X. Ding, X. Song, X. Chen, D. Ding, C. Xu and H. Chen, *Chemosphere*, 2022, **286**, DOI: 10.1016/j.chemosphere.2021.131720.

2 L. Qian, F. D. Kopinke, T. Scherzer, J. Griebel and A. Georgi, *Chem. Eng. J.*, 2022, **429**, DOI: 10.1016/j.cej.2021.132500.

3 Y. Yuan, L. Feng, X. He, X. Liu, N. Xie, Z. Ai, L. Zhang and J. Gong, *J. Hazard. Mater.*, 2022, **423**, DOI: 10.1016/j.jhazmat.2021.127176.

4 V. Méndez, S. Holland, S. Bhardwaj, J. McDonald, S. Khan, D. O'Carroll, R. Pickford, S. Richards, C. O'Farrell, N. Coleman, M. Lee and M. J. Manefield, *Sci. Total Environ.*, 2022, **829**, DOI: 10.1016/j.scitotenv.2022.154587.

5 B. Tansel, *J. Environ. Manage.*, 2022, **316**, 115291.

6 E. Hammel, T. F. Webster, R. Gurney and W. Heiger-Bernays, *iScience*, 2022, **25**, DOI: 10.1016/j.isci.2022.104020.

7 K. W. Pütz, S. Namazkar, M. Plassmann and J. P. Benskin, *Environ. Sci.:Processes Impacts*, 2022, **24**, DOI: 10.1039/d2em00123c.

8 S. Huang, M. Sima, Y. Long, C. Messenger and P. R. Jaffé, *J. Hazard. Mater.*, 2022, DOI: 10.1016/j.jhazmat.2021.127699.

9 M. Ruiz-Urigüen, W. Shuai, S. Huang and P. R. Jaffé, *Chemosphere*, 2022, DOI: 10.1016/j.chemosphere.2021.133506.

10 C. M. Butt, D. C. G. Muir and S. A. Mabury, *Environ. Toxicol. Chem.*, 2014, **33**, 243–267.

11 N. AlSawaftah, W. Abuwatfa, N. Darwish and G. Husseini, *Water*, 2021, **13**(9), 1327.

12 D. Lu, S. Sha, J. Luo, Z. Huang and X. Z. Jackie, *J. Hazard. Mater.*, 2020, **386**, 121963.

13 T. H. Kim, S. Yu, Y. Choi, T. Y. Jeong and S. D. Kim, *Sci. Total Environ.*, 2018, **631–632**, 1295–1303.

14 J. Shenglan, M. M. Dos Santos, C. Li and S. A. Snyder, *Anal. Bioanal. Chem.*, 2022, **414**(9), 2795–2807.

15 Per- and Polyfluoroalkyl Substances (PFAS), *US EPA*, https://www.epa.gov/sdwa/and-polyfluoroalkyl-substances-pfas, accessed 15 July 2024.

16 M. J. Gander, *Water Int.*, 2022, 1–23.

17 A. J. Lewis, X. Yun, D. E. Spooner, M. J. Kurz, E. R. McKenzie and C. M. Sales, *Sci. Total Environ.*, 2022, **822**, 153561.

18 J. O'Connor, N. S. Bolan, M. Kumar, A. S. Nitai, M. B. Ahmed, S. S. Bolan, M. Vithanage, J. Rinklebe, R. Mukhopadhyay, P. Srivastava, B. Sarkar, A. Bhatnagar, H. Wang, K. H. M. Siddique and M. B. Kirkham, *Process Saf. Environ. Prot.*, 2022, **164**, 91–108.

19 B. Saawarn, B. Mahanty, S. Hait and S. Hussain, *Environ. Res.*, 2022, **214**, 114004.

20 S. Kurwadkar, J. Dane, S. R. Kanel, M. N. Nadagouda, R. W. Cawdrey, B. Ambade, G. C. Struckhoff and R. Wilkin, *Sci. Total Environ.*, 2022, **809**, 151003.

21 D. Ma, H. Zhong, J. Lv, Y. Wang and G. Jiang, *J. Environ. Sci.*, 2022, **112**, 71–81.

22 M. Clara, C. Scheffknecht, S. Scharf, S. Weiss and O. Gans, *Water Sci. Technol.*, 2008, **58**, 59–66.

23 Z. Y. Yong, K. Y. Kim and J. E. Oh, *Environ. Pollut.*, 2021, **268**, 115395.

24 T. Schroeder, D. Bond and J. Foley, *Environ. Sci.:Processes Impacts*, 2021, **23**, 291–301.

25 M. G. Evich, M. J. B. Davis, J. P. McCord, B. Acrey, J. A. Awkerman, D. R. U. Knappe, A. B. Lindstrom, T. F. Speth, C. Tebes-Stevens, M. J. Strynar, Z. Wang, E. J. Weber, W. M. Henderson and J. W. Washington, *Science*, 2022, **375**, eabg9065.

26 L. G. T Gaines and C. G. Linda T Gaines, *Am. J. Ind. Med.*, 2022, **66**, DOI: 10.1002/AJIM.23362.

27 G. Glenn, R. Shogren, X. Jin, W. Orts, W. Hart-Cooper and L. Olson, *Compr. Rev. Food Sci. Food Saf.*, 2021, **20**, 2596–2625.

28 C. K. Ober, F. Käfer and J. Deng, *J. Micro/Nanopatterning, Mater., Metrol.*, 2022, **21**, 010901.

29 J. Glüge, M. Scheringer, I. T. Cousins, J. C. Dewitt, G. Goldenman, D. Herzke, R. Lohmann, C. A. Ng, X. Trier and Z. Wang, *Environ. Sci.:Processes Impacts*, 2020, **22**, 2345–2373.

30 K. Dasu, X. Xia, D. Siriwardena, T. P. Klupinski and B. Seay, *J. Environ. Manage.*, 2022, **301**, 113879.

31 K. J. Harris, G. Munoz, V. Woo, S. Sauvé and A. A. Rand, *Environ. Sci. Technol.*, 2022, **2022**, 14594–14604.

32 K. Pozo, L. B. Moreira, P. Karaskova, P. Přibylová, J. Klánová, M. U. de Carvalho, L. A. Maranho and D. M. de Souza Abessa, *Mar. Pollut. Bull.*, 2022, **182**, 113938.

33 A. Nickerson, A. C. Maizel, P. R. Kulkarni, D. T. Adamson, J. J. Kornuc and C. P. Higgins, *Environ. Sci. Technol.*, 2020, **54**, 4952–4962.

34 Å. Høisæter, A. Pfaff and G. D. Breedveld, *J. Contam. Hydrol.*, 2019, **222**, 112–122.

35 D. J. Muensterman, L. Cahuas, I. A. Titaley, C. Schmokel, F. B. De La Cruz, M. A. Barlaz, C. C. Carignan, G. F. Peaslee and J. A. Field, *Environ. Sci. Technol. Lett.*, 2022, **9**, 320–326.

36 T. Stoiber, S. Evans and O. V. Naidenko, *Chemosphere*, 2020, **260**, 127659.

37 E. Hepburn, C. Madden, D. Szabo, T. L. Coggan, B. Clarke and M. Currell, *Environ. Pollut.*, 2019, **248**, 101–113.

38 H. Hamid, L. Y. Li and J. R. Grace, *Environ. Pollut.*, 2018, **235**, 74–84.

39 T. L. Coggan, D. Moodie, A. Kolobaric, D. Szabo, J. Shimeta, N. D. Crosbie, E. Lee, M. Fernandes and B. O. Clarke, *Heliyon*, 2019, **5**, e02316.

40 S. P. Lenka, M. Kah and L. P. Padhye, *Water Res.*, 2021, **199**, 117187.

41 J. A. K. Silva, J. L. Guelfo, J. Šimůnek and J. E. McCray, *J. Contam. Hydrol.*, 2022, **251**, 104089.

42 L. B. Ebinezer, I. Battisti, N. Sharma, L. Ravazzolo, L. Ravi, A. R. Trentin, G. Barion, A. Panozzo, S. Dall'Acqua, T. Vamerali, S. Quaggiotti, G. Arrigoni and A. Masi, *J. Hazard. Mater.*, 2022, **438**, 129512.

43 J. Li, J. Sun and P. Li, *Environ. Int.*, 2022, **158**, 106891.

44 J. A. Padilla-Sánchez, E. Papadopoulou, S. Poothong and L. S. Haug, *Environ. Sci. Technol.*, 2017, **51**, 12836–12843.

45 K. L. Vorst, N. Saab, P. Silva, G. Curtzwiler and A. Steketee, *Trends Food Sci. Technol.*, 2021, **116**, 1203–1211.

46 J. L. Domingo and M. Nadal, *Environ. Res.*, 2019, **177**, 108648.

47 O. Ragnarsdóttir, M. A. E. Abdallah and S. Harrad, *Environ. Pollut.*, 2022, **307**, 119478.

48 K. J. Harris, G. Munoz, V. Woo, S. Sauvé and A. A. Rand, *Environ. Sci. Technol.*, 2022, **2022**, 14594–14604.

49 Stockholm convention, All POPs listed in the Stockholm Convention, **http://chm.pops.int/TheConvention/ThePOPs/ListingofPOPs/tabid/2509/Default.aspx**, accessed 22 November 2022.

50 J. Falandysz, B. Jiménez and S. Taniyasu, *Chemosphere*, 2022, **291**, 132876.

51 S. E. Fenton, A. Ducatman, A. Boobis, J. C. DeWitt, C. Lau, C. Ng, J. S. Smith and S. M. Roberts, *Environ. Toxicol. Chem.*, 2021, **40**, 606–630.

52 J. Li, J. Sun and P. Li, *Environ. Int.*, 2022, **158**, 106891.

53 X. Hu, S. Li, P. M. Cirillo, N. Y. Krigbaum, V. L. Tran, D. P. Jones and B. A. Cohn, *Reprod. Toxicol.*, 2020, **92**, 120–128.

54 Q. Cui, Y. Pan, J. Wang, H. Liu, B. Yao and J. Dai, *Environ. Pollut.*, 2020, **266**, DOI: **10.1016/j.envpol.2020.115330**.

55 C. J. Chang, D. B. Barr, Q. Zhang, A. L. Dunlop, M. M. Smarr, K. Kannan, P. Panuwet, V. Tangpricha, L. Shi, D. Liang, E. J. Corwin and P. B. Ryan, *Environ. Res.*, 2021, **202**, 111713.

56 S. Liu, N. Yin and F. Faiola, *Environ. Sci. Technol. Lett.*, 2018, **5**, 237–242.

57 X. Han, L. Meng, G. Zhang, Y. Li, Y. Shi, Q. Zhang and G. Jiang, *Environ. Int.*, 2021, **156**, 106637.

58 A. J. Blomberg, Y. H. Shih, C. Messerlian, L. H. Jørgensen, P. Weihe and P. Grandjean, *Environ. Res.*, 2021, **200**, 111400.

59 Y. Fan, X. Li, Q. Xu, Y. Zhang, X. Yang, X. Han, G. Du, Y. Xia, X. Wang and C. Lu, *Environ. Pollut.*, 2020, **266**, 115138.

60 Y. T. Zhang, M. Zeeshan, F. Su, Z. M. Qian, S. Dee Geiger, S. Edward McMillin, Z. Bin Wang, P. X. Dong, Y. Q. Ou, S. M. Xiong, X. B. Shen, P. E. Zhou, B. Y. Yang, C. Chu, Q. Q. Li, X. W. Zeng, W. R. Feng, Y. Z. Zhou and G. H. Dong, *Environ. Int.*, 2022, **158**, 106913.

61 A. L. Bjorke-Monsen, K. Varsi, M. Averina, J. Brox and S. Huber, *BMJ Nutr Prev Health*, 2020, **3**, 277.

62 A. F. Ojo, Q. Xia, C. Peng and J. C. Ng, *Chemosphere*, 2021, **281**, 130808.

63 M. Jabeen, M. Fayyaz and J. Irudayaraj, *Toxics*, 2020, **8**, 112.

64 J. Wang, Y. Pan, Q. Cui, B. Yao, J. Wang and J. Dai, *Environ. Sci. Technol.*, 2018, **52**, 13553–13561.

65 T. L. Alderete, R. Jin, D. I. Walker, D. Valvi, Z. Chen, D. P. Jones, C. Peng, F. D. Gilliland, K. Berhane, D. V. Conti, M. I. Goran and L. Chatzi, *Environ. Int.*, 2019, **126**, 445–453.

66 Z. Chen, T. Yang, D. I. Walker, D. C. Thomas, C. Qiu, L. Chatzi, T. L. Alderete, J. S. Kim, D. V. Conti, C. V. Breton, D. Liang, E. R. Hauser, D. P. Jones and F. D. Gilliland, *Environ. Int.*, 2020, **145**, 106091.

67 S. Zhang, K. Chen, W. Li, Y. Chai, J. Zhu, B. Chu, N. Li, J. Yan, S. Zhang and Y. Yang, *Environ. Int.*, 2021, **156**, 106745.

68 E. Papadopoulou, N. Stratakis, X. Basagaña, A. L. Brantsæter, M. Casas, S. Fossati, R. Gražulevičienė, L. Småstuen Haug, B. Heude, L. Maitre, R. R. C. McEachan, O. Robinson, T. Roumeliotaki, E. Sabidó, E. Borràs, J. Urquiza, M. Vafeiadi, Y. Zhao, R. Slama, J. Wright, D. V. Conti, M. Vrijheid and L. Chatzi, *Environ. Int.*, 2021, **157**, 106853.

69 A. A. Banjabi, A. J. Li, T. A. Kumosani, J. M. Yousef and K. Kannan, *Environ. Res.*, 2020, **187**, 109676.

70 H. Gardener, Q. Sun and P. Grandjean, *Environ. Res.*, 2021, **192**, 110287.

71 Y. R. Kim, N. White, J. Bräunig, S. Vijayasarathy, J. F. Mueller, C. L. Knox, F. A. Harden, R. Pacella and L. M. L. Toms, *Environ. Res.*, 2020, **190**, 109963.

72 R. C. Wiener and C. Waters, *J. Publ. Health Dent.*, 2019, **79**, 307–319.

73 Q. Chen, X. Zhang, Y. Zhao, W. Lu, J. Wu, S. Zhao, J. Zhang and L. Huang, *Chemosphere*, 2019, **226**, 17–23.

74 K. Y. Gebreab, M. N. H. Eeza, T. Bai, Z. Zuberi, J. Matysik, K. E. O'Shea, A. Alia and J. P. Berry, *Environ. Pollut.*, 2020, **265**, 114928.

75 L. M. Labine, E. A. Oliveira Pereira, S. Kleywegt, K. J. Jobst, A. J. Simpson and M. J. Simpson, *Environ. Res.*, 2022, **212**, 113582.

76 N. Kotlarz, J. McCord, D. Collier, C. Suzanne Lea, M. Strynar, A. B. Lindstrom, A. A. Wilkie, J. Y. Islam, K. Matney, P. Tarte, M. E. Polera, K. Burdette, J. Dewitt,

K. May, R. C. Smart, D. R. U. Knappe and J. A. Hoppin, *Environ. Health Perspect.*, 2020, **128**, 1–12.

77 J. P. Antignac, B. Veyrand, H. Kadar, P. Marchand, A. Oleko, B. Le Bizec and S. Vandentorren, *Chemosphere*, 2013, **91**, 802–808.

78 Y. Lu, L. Meng, D. Ma, H. Cao, Y. Liang, H. Liu, Y. Wang and G. Jiang, *Environ. Pollut.*, 2021, **273**, 116460.

79 E. Piva, P. Fais, G. Cecchetto, M. Montisci, G. Viel and J. P. Pascali, *J. Chromatogr. B*, 2021, **1172**, 122651.

80 B. A. Cohn, M. A. La Merrill, N. Y. Krigbaum, M. Wang, J. S. Park, M. Petreas, G. Yeh, R. C. Hovey, L. Zimmermann and P. M. Cirillo, *Reprod. Toxicol.*, 2020, **92**, 112–119.

81 Y. R. Kim, N. White, J. Bräunig, S. Vijayasarathy, J. F. Mueller, C. L. Knox, F. A. Harden, R. Pacella and L. M. L. Toms, *Environ. Res.*, 2020, **190**, 109963.

82 C. J. Chang, D. B. Barr, Q. Zhang, A. L. Dunlop, M. M. Smarr, K. Kannan, P. Panuwet, V. Tangpricha, L. Shi, D. Liang, E. J. Corwin and P. B. Ryan, *Environ. Res.*, 2021, **202**, 111713.

83 Y. Fan, X. Li, Q. Xu, Y. Zhang, X. Yang, X. Han, G. Du, Y. Xia, X. Wang and C. Lu, *Environ. Pollut.*, 2020, **266**, 115138.

84 X. Han, L. Meng, G. Zhang, Y. Li, Y. Shi, Q. Zhang and G. Jiang, *Environ. Int.*, 2021, **156**, 106637.

85 Z. Chen, T. Yang, D. I. Walker, D. C. Thomas, C. Qiu, L. Chatzi, T. L. Alderete, J. S. Kim, D. V. Conti, C. V. Breton, D. Liang, E. R. Hauser, D. P. Jones and F. D. Gilliland, *Environ. Int.*, 2020, **145**, 106091.

86 S. Zhang, K. Chen, W. Li, Y. Chai, J. Zhu, B. Chu, N. Li, J. Yan, S. Zhang and Y. Yang, *Environ. Int.*, 2021, **156**, 106745.

87 P. M. Lind, S. Salihovic, B. van Bavel and L. Lind, *Environ. Res.*, 2017, **152**, 157–164.

88 A. A. Banjabi, A. J. Li, T. A. Kumosani, J. M. Yousef and K. Kannan, *Environ. Res.*, 2020, **187**, 109676.

89 Q. Cui, Y. Pan, J. Wang, H. Liu, B. Yao and J. Dai, *Environ. Pollut.*, 2020, **266**, DOI: 10.1016/J.ENVPOL.2020.115330.

90 J. J. Shearer, C. L. Callahan, A. M. Calafat, W. Y. Huang, R. R. Jones, V. S. Sabbisetti, N. D. Freedman, J. N. Sampson, D. T. Silverman, M. P. Purdue and J. N. Hofmann, *J. Natl. Cancer Inst.*, 2021, **113**, 580–587.

91 O. B. Imir, A. Z. Kaminsky, Q. Y. Zuo, Y. J. Liu, R. Singh, M. J. Spinella, J. Irudayaraj, W. Y. Hu, G. S. Prins and Z. M. Erdogan, *Nutrients*, 2021, **13**, 3902.

92 B. P. Rickard, X. Tan, S. E. Fenton and I. Rizvi, *Int. J. Mol. Sci.*, 2022, **23**, 5176.

93 K. Roth and M. C. Petriello, *Front. Endocrinol.*, 2022, **13**, 1796.

94 R. Ghisi, T. Vamerali and S. Manzetti, *Environ. Res.*, 2019, **169**, 326–341.

95 L. Zhou, M. Xia, L. Wang and H. Mao, *Chemosphere*, 2016, **159**, 420–425.

96 W. Zhang and Y. Liang, *Chemosphere*, 2021, **276**, 130165.

97 A. K. Sivaram, P. Logeshwaran, A. Surapaneni, K. Shah, N. Crosbie, Z. Rogers, E. Lee, K. Venkatraman, K. Kannan, R. Naidu and M. Megharaj, *Environ. Toxicol. Chem.*, 2021, **40**, 792–798.

98 P. Li, Z. Xiao, J. Sun, X. Oyang, X. Xie, Z. Li, X. Tian and J. Li, *Sci. Total Environ.*, 2020, **726**, 138382.

99 R. Drew, T. G. Hagen and D. Champness, *Food Addit. Contam.,:Part A*, 2021, **38**(11), 1897–1913.

100 P. C. Bost, M. J. Strynar, J. L. Reiner, J. A. Zweigenbaum, P. L. Secoura, A. B. Lindstrom and J. A. Dye, *Environ. Res.*, 2016, **151**, 145–153.

101 E. Zafeiraki, I. Vassiliadou, D. Costopoulou, L. Leondiadis, H. A. Schafft, R. L. A. P. Hoogenboom and S. P. J. van Leeuwen, *Chemosphere*, 2016, **156**, 280–285.

102 R. Vestergren, F. Orata, U. Berger and I. T. Cousins, *Environ. Sci. Pollut. Res.*, 2013, **20**, 7959–7969.

103 A. V. Jacobsen, M. Nordén, M. Engwall and N. Scherbak, *Environ. Sci. Pollut. Res.*, 2018, **25**, 23074–23081.

104 X. Duan, W. Sun, H. Sun and L. Zhang, *Environ. Pollut.*, 2021, **278**, 116840.

105 R. M. Foguth, R. W. Flynn, C. de Perre, M. Iacchetta, L. S. Lee, M. S. Sepúlveda and J. R. Cannon, *Toxicol. Appl. Pharmacol.*, 2019, **377**, 114623.

106 C. A. McDonough, C. Ward, Q. Hu, S. Vance, C. P. Higgins and J. C. DeWitt, *Toxicol. Sci.*, 2020, **178**, 104–114.

107 H. F. Berntsen, C. G. Bjørklund, J. N. Audinot, T. Hofer, S. Verhaegen, E. Lentzen, A. C. Gutleb and E. Ropstad, *Neurotoxicology*, 2017, **63**, 70–83.

108 P. Song, D. Li, X. Wang and X. Zhong, *Andrologia*, 2018, **50**, e13059.

109 J. Liu, X. Zhao, Y. Liu, X. Qiao, X. Wang, M. Ma, X. Jin, C. Liu, B. Zheng, J. Shen and R. Guo, *Ecotoxicol. Environ. Saf.*, 2019, **182**, 109454.

110 N. H. Lam, C. R. Cho, J. S. Lee, H. Y. Soh, B. C. Lee, J. A. Lee, N. Tatarozako, K. Sasaki, N. Saito, K. Iwabuchi, K. Kannan and H. S. Cho, *Sci. Total Environ.*, 2014, **491–492**, 154–162.

111 T. C. Guillette, J. McCord, M. Guillette, M. E. Polera, K. T. Rachels, C. Morgeson, N. Kotlarz, D. R. U. Knappe, B. J. Reading, M. Strynar and S. M. Belcher, *Environ. Int.*, 2020, **136**, 105358.

112 Y. Rericha, D. Cao, L. Truong, M. Simonich, J. A. Field and R. L. Tanguay, *Chem. Res. Toxicol.*, 2021, **34**, 1409–1416.

113 K. Y. Gebreab, M. N. H. Eeza, T. Bai, Z. Zuberi, J. Matysik, K. E. O'Shea, A. Alia and J. P. Berry, *Environ. Pollut.*, 2020, **265**, 114928.

114 P. Chen, J. Yang, G. Chen, S. Yi, M. Liu and L. Zhu, *Environ. Sci. Technol. Lett.*, 2020, **7**, 330–336.

115 G. Shi, Q. Cui, H. Zhang, R. Cui, Y. Guo and J. Dai, *Chem. Res. Toxicol.*, 2019, **32**, 1432–1440.

116 A. C. Soloff, B. J. Wolf, N. D. White, D. Muir, S. Courtney, G. Hardiman, G. D. Bossart and P. A. Fair, *J. Appl. Toxicol.*, 2017, **37**, 1108–1116.

117 K. Y. Gebreab, M. N. H. Eeza, T. Bai, Z. Zuberi, J. Matysik, K. E. O'Shea, A. Alia and J. P. Berry, *Environ. Pollut.*, 2020, **265**, 114928.

118 M. Dadashi Firouzjaei, E. Zolghadr, S. Ahmadalipour, N. Taghvaei, F. Akbari Afkhami, S. Nejati and M. A. Elliott, *Environ. Chem. Lett.*, 2021, **20**(1), 661–679.

119 X. Z. Niu, L. Abrell, R. Sierra-Alvarez, J. A. Field and J. Chorover, *J. Chromatogr. A*, 2022, **1664**, 462817.

120 S. Taniyasu, L. W. Y. Yeung, H. Lin, E. Yamazaki, H. Eun, P. K. S. Lam and N. Yamashita, *Chemosphere*, 2022, **288**, 132440.

121 X. Bai and Y. Son, *Sci. Total Environ.*, 2021, **751**, 141622.

122 T. Sanan and M. Magnuson, *J. Chromatogr. A*, 2020, **1626**, 461324.

123 J. de Jong, V. Schoemann, D. Lannuzel, J. L. Tison and N. Mattielli, *Anal. Chim. Acta*, 2008, **623**, 126–139.

124 S. Wolf, C. Grochow, S. Porcher and B. Mader, *AGUFM*, 2019, **2019**, GH11B–1041.

125 Z. Xin, C. Qiu, R. Ullah, and Y. Liu, Using Automated Solid Phase Extractio n and LC-MS/MS, Thermo Fisher Scientific, Sunnyvale, CA 73883, 2020.

126 L. J. Winchell, M. J. M. Wells, J. J. Ross, X. Fonoll, J. W. Norton, S. Kuplicki, M. Khan and K. Y. Bell, *Sci. Total Environ.*, 2021, **774**, 145257.

127 J. Janda, K. Nödler, H. J. Brauch, C. Zwiener and F. T. Lange, *Environ. Sci. Pollut. Res.*, 2019, **26**, 7326–7336.

128 J. Borrull, A. Colom, J. Fabregas, E. Pocurull and F. Borrull, *J. Chromatogr. A*, 2020, **1629**, 461485.

129 U. Eriksson, P. Haglund and A. Kärrman, *J. Environ. Sci.*, 2017, **61**, 80–90.

130 M. al Amin, Z. Sobhani, Y. Liu, R. Dharmaraja, S. Chadalavada, R. Naidu, J. M. Chalker and C. Fang, *Environ. Technol. Innov.*, 2020, **19**, 100879.

131 J. Janda, K. Nödler, H. J. Brauch, C. Zwiener and F. T. Lange, *Environ. Sci. Pollut. Res.*, 2019, **26**, 7326–7336.

132 S. Castiglioni, S. Valsecchi, S. Polesello, M. Rusconi, M. Melis, M. Palmiotto, A. Manenti, E. Davoli and E. Zuccato, *J. Hazard. Mater.*, 2015, **282**, 51–60.

133 V. Mulabagal, L. Liu, J. Qi, C. Wilson and J. S. Hayworth, *Talanta*, 2018, **190**, 95–102.

134 Y. Liu, A. D. S. Pereira and J. W. Martin, *Anal. Chem.*, 2015, **87**, 4260–4268.

135 M. Sörengård, S. Bergström, P. McCleaf, K. Wiberg and L. Ahrens, *Environ. Pollut.*, 2022, **311**, 119981.

136 M. A. Mottaleb, Q. X. Ding, K. G. Pennell, E. N. Haynes and A. J. Morris, *J. Chromatogr. A*, 2021, **1653**, 462426.

137 C. S. Skaggs and B. A. Logue, *J. Chromatogr. A*, 2021, **1659**, 462493.

138 V. Boiteux, C. Bach, V. Sagres, H. Jessica, A. Colin, C. Rosin, J.-F. Munoz and D. Xavier, *Int. J. Environ. Anal. Chem.*, 2016, **96**(8), 705–728.

139 V. A. Nikiforov, *Chemosphere*, 2021, **276**, 130044.

140 C. Bach, X. Dauchy, V. Boiteux, A. Colin, J. Hemard, V. Sagres, C. Rosin and J. F. Munoz, *Environ. Sci. Pollut. Res.*, 2017, **24**, 4916–4925.

141 E. von Abercron, S. Falk, T. Stahl, S. Georgii, G. Hamscher, H. Brunn and F. Schmitz, *Sci. Total Environ.*, 2019, **673**, 384–391.

142 E. F. Houtz and D. L. Sedlak, *Environ. Sci. Technol.*, 2012, **46**, 9342–9349.

143 V. Khosravi, F. Doulati Ardejani, A. Gholizadeh and M. Saberioon, *Remote Sensing*, 2021, **13**, 1277.

144 J. C. Ritchie, C. M. Cooper and F. R. Schiebe, *Remote Sens. Environ.*, 1990, **33**, 137–148.

145 J. Xue and B. Su, *J. Sens.*, 2017, DOI: **10.1155/2017/1353691**.

146 F. Mohseni, F. Saba, S. M. Mirmazloumi, M. Amani, M. Mokhtarzade, S. Jamali and S. Mahdavi, *Mar. Environ. Res.*, 2022, **180**, 105701.

147 S. Lamine, G. P. Petropoulos, P. A. Brewer, N. E. I. Bachari, P. K. Srivastava, K. Manevski, C. Kalaitzidis and M. G. Macklin, *Sensors*, 2019, **19**, 762.

148 T. Stoiber, S. Evans and V. N. Olga, *Chemosphere*, 2020, **260**, 127659.

149 L. J. Winchell, J. J. Ross, M. J. Wells, X. Fonoll, Norton and K. Y. Bell, *Water Environ. Res.*, 2021, **93**(6), 826–843.

150 G. K. Longendyke, S. Katel and Y. Wang, *Environ. Sci.:Processes Impacts*, 2022, **24**(2), 196–208.

151 J. Yu, A. Nickerson, Y. Li, Y. Fang and T. J. Strathmann, *Environ. Sci.*, 2020, **6**, 1388–1399.

152 J. T. McDonough, J. Kirby, C. Bellona, J. A. Quinnan, N. Welty, J. Follin and K. Liberty, *Remediation*, 2022, **32**, 75–90.

153 T. D. Appleman, C. P. Higgins, O. Quiñones, B. J. Vanderford, C. Kolstad, J. C. Zeigler-Holady and E. R. V. Dickenson, *Water Res.*, 2014, **51**, 246–255.

154 J. Metz, P. Zuo, B. Wang, M. S. Wong and P. J. J. Alvarez, *Environ. Sci. Technol. Lett.*, 2022, **9**, 673–679.

155 Y. J. Lei, Y. Tian, Z. Sobhani, R. Naidu and C. Fang, *Chem. Eng. J.*, 2020, DOI: **10.1016/j.cej.2020.124215**.

156 J. Radjenovic, N. Duinslaeger, S. S. Avval and B. P. Chaplin, *Am. Chem. Soc.*, 2020, **54**, DOI: **10.1021/acs.est.0c06212**.

157 M. F. Rahman, S. Peldszus and W. B. Anderson, *Water Res.*, 2014, **50**, 318–340.

158 J. K. Johnson, C. M. Hoffman, D. A. Smith and Z. Xia, *ACS Omega*, 2019, **4**, 8001–8006.

159 C. Boo, Y. Wang, I. Zucker, Y. Choo, C. O. Osuji and M. Elimelech, *Environ. Sci. Technol.*, 2018, **52**, 7279–7288.

160 T. Jin, M. Peydayesh, H. Joerss, J. Zhou, S. Bolisetty and R. Mezzenga, *Environ. Sci.*, 2021, **7**, 1873–1884.

161 S. El Meragawi, A. Akbari, S. Hernandez, M. S. Mirshekarloo, D. Bhattacharyya, A. Tanksale and M. Majumder, *J. Mater. Chem. A*, 2020, **8**, 24800–24811.

162 Y. Zheng, F. Rao, M. Zhang, J. Li and W. Huang, *Clean Eng. Technol.*, 2021, 100344.

163 T. Le, E. Jamshidi, M. Beidaghi and M. R. Esfahani, *ACS Appl. Mater. Interfaces*, 2022, **14**, 25397–25408.

164 K. Zarshenas, H. Dou, S. Habibpour, A. Yu and Z. Chen, *ACS Appl. Mater. Interfaces*, 2022, **14**, 1838–1849.

165 J. Eke, L. Banks, M. A. Mottaleb, A. J. Morris, O. V Tsyusko and I. C. Escobar, *Membranes*, 2021, **11**, 1–18.

166 C. Zhao, G. Hu, D. Hou, L. Yu, Y. Zhao, J. Wang, A. Cao and Y. Zhai, *Sep. Purif. Technol.*, 2018, **202**, 385–396.

167 C. J. Liu, T. J. Strathmann and C. Bellona, *Water Res.*, 2020, DOI: **10.1016/j.watres.2020.116546**.

168 E. Steinle-Darling and M. Reinhard, *Environ. Sci. Technol.*, 2008, **42**, 5292–5297.

169 C. Y. Tang, Q. S. Fu, A. P. Robertson, C. S. Criddle and J. O. Leckie, *Environ. Sci. Technol.*, 2006, **40**, 7343–7349.

170 X. B. Gong and Z. W. He, *Water Air Soil Pollut.*, 2021, **232**, 215.

171 C. Baudequin, Z. Mai, M. Rakib, I. Deguerry, R. Severac, M. Pabon and E. Couallier, *J. Membr. Sci.*, 2014, **458**, 111–119.

172 M. Hassan, Y. Liu, R. Naidu, J. Du and F. Qi, *Environ. Technol. Innov.*, 2020, DOI: **10.1016/j.eti.2020.100816**.

173 D. Zhang, Q. He, M. Wang, W. Zhang and Y. Liang, *Environ. Technol.*, 2021, **42**, 1798–1809.

174 F. Dixit, B. Barbeau, S. G. Mostafavi and M. Mohseni, *Water Res.*, 2020, DOI: **10.1016/j.watres.2020.116098**.

175 G. Erica, M. Sgroi, P. P. Falciglia, F. G. A. Vagliasindi and P. Roccaro, *Water Res.*, 2020, **171**, 115381.

176 L. Qian, F. D. Kopinke and A. Georgi, *Environ. Sci. Technol.*, 2021, **55**, 614–622.

177 J. Cui, P. Gao and Y. Deng, *Am. Chem. Soc.*, 2020, **54**, 3752–3766.

178 D. Wu, X. Li, J. Zhang, W. Chen, P. Lu, Y. Tang and L. Li, *Sep. Purif. Technol.*, 2018, **207**, 255–261.

179 S. Verma, B. Mezgebe, E. Sahle-Demessie and M. N. Nadagouda, *Chemosphere*, 2021, DOI: **10.1016/j.chemosphere.2021.130660**.

180 J. Wang, C. Cao, Y. Zhang, Y. Zhang and L. Zhu, *Appl. Catal., B*, 2021, DOI: **10.1016/j.apcatb.2021.119911**.

181 C. J. Liu, G. McKay, D. Jiang, R. Tenorio, J. T. Cath, C. Amador, C. C. Murray, J. B. Brown, H. B. Wright, C. Schaefer, C. P. Higgins, C. Bellona and T. J. Strathmann, *Water Res.*, 2021, DOI: **10.1016/j.watres.2021.117677**.

182 S. S. R. K. C. Yamijala, R. Shinde and B. M. Wong, *Phys. Chem. Chem. Phys.*, 2020, **22**, 6804–6808.

183 M. Trojanowicz, I. Bartosiewicz, A. Bojanowska-Czajka, T. Szreder, K. Bobrowski, G. Nałęcz-Jawecki, S. Męczyńska-Wielgosz and H. Nichipor, *Chem. Eng. J.*, 2019, DOI: **10.1016/j.cej.2019.122303**.

184 M. H. Kim, N. Wang and K. H. Chu, *Appl. Microbiol. Biotechnol.*, 2014, **98**, 1831–1840.

185 T. F. Mastropietro, R. Bruno, E. Pardo and D. Armentano, *Dalton Trans.*, 2021, **50**, 5398–5410.

186 M. N. Nadagouda and T. Lee, *Am. Chem. Soc.*, 2021, **2**, DOI: **10.1021/accountsmr.0c00106**.

187 Y. Zhou, Z. He, Y. Tao, Y. Xiao, T. Zhou, T. Jing, Y. Zhou and S. Mei, *Chem. Eng. J.*, 2016, **303**, 156–166.

188 C. Zhao, C. Y. Tang, P. Li, P. Adrian and G. Hu, *J. Membr. Sci.*, 2016, **503**, 31–41.

189 L. Xiao, Y. Ling, A. Alsbaiee, C. Li, D. E. Helbling and W. R. Dichtel, *J. Am. Chem. Soc.*, 2017, **139**, 7689–7692.

190 E. Gagliano, M. Sgroi, P. P. Falciglia, F. G. Vagliasindi and P. Roccaro, *Water Res.*, 2020, **171**, 115381.

191 M. Inyang and E. R. V. Dickenson, *Chemosphere*, 2017, **184**, 168–175.

192 Q. Yu, S. Deng and G. Yu, *Water Res.*, 2008, **42**, 3089–3097.

193 M. Park, S. Wu, I. J. Lopez, J. Y. Chang, T. Karanfil and S. A. Snyder, *Water Res.*, 2020, **170**, 115364.

194 W. Chen, X. Zhang, M. Mamadiev and Z. Wang, *RSC Adv.*, 2017, **7**, 927–938.

195 D. P. Siriwardena, M. Crimi, T. M. Holsen, C. Bellona, C. Divine and E. Dickenson, *Environ. Eng. Sci.*, 2019, **36**, 453–465.

196 C. C. Murray, H. Vatankhah, C. A. McDonough, A. Nickerson, T. T. Hedtke, T. Y. Cath, C. P. Higgins and C. L. Bellona, *J. Hazard. Mater.*, 2019, **366**, 160–168.

197 Q. Zhou, S. Deng, Q. Zhang, Q. Fan, J. Huang and G. Yu, *Chemosphere*, 2010, **81**, 453–458.

198 C. Wu, M. J. Klemes, B. Trang, W. R. Dichtel and D. E. Helbling, *Water Res.*, 2020, **182**, 115950.

199 C. A. Clark, K. N. Heck, C. D. Powell and M. S. Wong, *ACS Sustain. Chem. Eng.*, 2019, **7**, 6619–6628.

200 M. Ateia, M. Arifuzzaman, S. Pellizzeri, M. F. Attia, N. Tharayil, J. N. Anker and T. Karanfil, *Water Res.*, 2019, **163**, 114874.

201 M. Ateia, M. F. Attia, A. Maroli, N. Tharayil, F. Alexis, D. C. Whitehead and T. Karanfil, *Environ. Sci. Technol. Lett.*, 2018, **5**, 764–769.

202 W. Ji, L. Xiao, Y. Ling, C. Ching, M. Matsumoto, R. P. Bisbey, D. E. Helbling and W. R. Dichtel, *J. Am. Chem. Soc.*, 2018, **140**, 12677–12681.

203 E. Kumarasamy, I. M. Manning, L. B. Collins, O. Coronell and F. A. Leibfarth, *ACS Cent. Sci.*, 2020, **6**, 487–492.

204 C. Ching, M. J. Klemes, B. Trang, W. R. Dichtel and D. E. Helbling, *Environ. Sci. Technol.*, 2020, **54**, 12693–12702.

205 J. Huo, X. Min, Q. Dong, S. Xu and Y. Wang, *Chemosphere*, 2022, **287**, 132297.

206 R. Li, S. Alomari, R. Stanton, M. C. Wasson, T. Islamoglu, O. K. Farha, T. M. Holsen, S. M. Thagard, D. J. Trivedi and M. Wriedt, *Chem. Mater.*, 2021, **33**, 3276–3285.

207 C. Zhao, Y. Xu, F. Xiao, J. Ma, Y. Zou and W. Tang, *Chem. Eng. J.*, 2021, **406**, 126852.

208 H. Konno, Y. Nakasaka, K. Yasuda, M. Omata and T. Masuda, *Catal. Today*, 2020, **352**, 220–226.

209 S. Y. Ma, J. Wang, L. Fan, H. L. Duan and Z. Q. Zhang, *J. Chromatogr. A*, 2020, **1611**, 460616.

210 L. H. Mohd Azmi, D. R. Williams and B. P. Ladewig, *Chemosphere*, 2021, **262**, 128072.

211 H. N. P. Vo, T. M. H. Nguyen, H. H. Ngo, W. Guo and P. Shukla, *Chemosphere*, 2022, **286**, 131622.

212 S. Kundu, S. Patel, P. Halder, T. Patel, M. Hedayati Marzbali, B. K. Pramanik, J. Paz-Ferreiro, C. C. De Figueiredo, D. Bergmann, A. Surapaneni, M. Megharaj and K. Shah, *Environ. Sci.*, 2021, **7**, 638–649.

213 Y. Wu, L. Qi and G. Chen, *J. Clean. Prod.*, 2022, **340**, 130742.

214 K. M. Krahn, G. Cornelissen, G. Castro, H. P. H. Arp, A. G. Asimakopoulos, R. Wolf, R. Holmstad, A. R. Zimmerman and E. Sørmo, *J. Hazard. Mater.*, 2022, 130449.

215 A. H. M. A. Sadmani, R. C. Andrews and D. M. Bagley, *J. Water Proc. Eng.*, 2014, **2**, 63–70.

216 V. Franke, M. Ullberg, P. McCleaf, M. Wålinder, S. J. Köhler and L. Ahrens, *ACS ES&T Water*, 2021, **1**, 782–795.

217 Á. Soriano, D. Gorri and A. Urtiaga, *Ind. Eng. Chem. Res.*, 2019, **58**, 3329–3338.

218 T. D. Appleman, E. R. V. Dickenson, C. Bellona and C. P. Higgins, *J. Hazard. Mater.*, 2013, **260**, 740–746.

219 M. Mon, R. Bruno, J. Ferrando-Soria, D. Armentano and E. Pardo, *J. Mater. Chem. A*, 2018, **6**(12), 4912–4947.

220 H. Deng, C. J. Doonan, H. Furukawa, R. B. Ferreira, J. Towne, C. B. Knobler, B. Wang and O. M. Yaghi, *Science*, 2010, **327**, 846–850.

221 C. Zhao, Y. Xu, F. Xiao, J. Ma, Y. Zou and W. Tang, *Chem. Eng. J.*, 2020, DOI: **10.1016/j.cej.2020.126852**.

222 M. N. Pervez, T. Jiang and Y. Liang, *J. Water Process Eng.*, 2024, **63**, 105471.

223 F. E. Ahmed, R. Hashaikeh and N. Hilal, *Desalination*, 2020, **495**, 114659.

224 J. Thompson, G. Eaglesham, J. Reungoat, Y. Poussade, M. Bartkow, M. Lawrence and J. F. Mueller, *Chemosphere*, 2011, **82**, 9–17.

225 M. N. Taher, S. A. Al-Mutwalli, S. Barisci, D. Y. Koseoglu-Imer, L. F. Dumée and M. M. A. Shirazi, *J. Water Process Eng.*, 2024, **59**, 104858.

226 J. Wang, C. Cao, Y. Wang, Y. Wang, B. Sun and L. Zhu, *Chem. Eng. J.*, 2019, DOI: **10.1016/j.cej.2019.123530**.

227 B. Xu, J. L. Zhou, A. Altaee, M. B. Ahmed, M. A. H. Johir, J. Ren and X. Li, *Chemosphere*, 2019, DOI: **10.1016/j.chemosphere.2019.124722**.

228 C. V. Reddy, R. Kumar, P. Chakrabortty, B. Karmakar, S. Pottipati, A. Kundu and B.-H. Jeon, *Chem. Eng. J.*, 2024, **492**, 152272.

229 Y. Yuan, L. Feng, X. He, X. Liu, N. Xie, Z. Ai, L. Zhang and J. Gong, *J. Hazard. Mater.*, 2022, **423**, 127176.

230 T. H. Kim, S. H. Lee, H. Y. Kim, K. Doudrick, S. Yu and S. D. Kim, *Chem. Eng. J.*, 2019, **361**, 1363–1370.

231 N. Wang, H. Lv, Y. Zhou, L. Zhu, Y. Hu, T. Majima and H. Tang, *Environ. Sci. Technol.*, 2019, **53**, 8302–8313.

232 B. Xu, J. L. Zhou, A. Altaee, M. B. Ahmed, M. A. H. Johir, J. Ren and X. Li, *Chemosphere*, 2020, **239**, 124722.

233 J. H. Carey, J. Lawrence and H. M. Tosine, *Bull. Environ. Contam. Toxicol.*, 1976, **16**, 697–701.

234 C. Chen, Q. Ma, F. Liu, J. Gao, X. Li, S. Sun, H. Yao, C. Liu, J. Young and W. Zhang, *J. Hazard. Mater.*, 2021, **419**, 126452.

235 Y. Zhu, T. Xu, D. Zhao, F. Li, W. Liu, B. Wang and B. An, *Chem. Eng. J.*, 2021, **421**, 129676.

236 R. Tenorio, J. Liu, X. Xiao, A. Maizel, C. P. Higgins, C. E. Schaefer and T. J. Strathmann, *Environ. Sci. Technol.*, 2020, **54**, 6957–6967.

237 I. Abusallout, J. Wang and D. Hanigan, *Environ. Sci.*, 2021, **7**, 1552–1562.

238 R. K. Singh, E. Brown, S. Mededovic Thagard and T. M. Holsen, *J. Hazard. Mater.*, 2021, **408**, 124452.

239 R. J. Wood, T. Sidnell, I. Ross, J. McDonough, J. Lee and M. J. Bussemaker, *Ultrason. Sonochem.*, 2020, **68**, 105196.

240 V. Franke, M. D. Schäfers, J. J. Lindberg and L. Ahrens, *Environ. Sci.*, 2019, **5**, 1887–1896.

241 K. Londhe, C. S. Lee, Y. Zhang, S. Grdanovska, T. Kroc, C. A. Cooper and A. K. Venkatesan, *ACS ES&T Water*, 2022, **1**, 827–841.

242 M. Park, S. Wu, I. J. Lopez, J. Y. Chang, T. Karanfil and S. A. Snyder, *Water Res.*, 2020, **170**, 115364.

243 Y. Yao, K. Volchek, C. E. Brown, A. Robinson and T. Obal, *Water Sci. Technol.*, 2014, **70**, 1983–1991.

244 C. Yuan, Y. Huang, F. S. Cannon and Z. Zhao, *J. Environ. Sci.*, 2020, **98**, 94–102.

245 F. Dixit, B. Barbeau and M. Mohseni, *Water Sci. Technol. Water Supply*, 2020, **20**, 3107–3119.

246 R. Wang, C. Ching, W. R. Dichtel and D. E. Helbling, *Environ. Sci. Technol. Lett.*, 2020, **7**, 954–960.

247 F. Xiao, B. Jin, S. A. Golovko, M. Y. Golovko and B. Xing, *Environ. Sci. Technol.*, 2019, **53**, 11818–11827.

248 F. Dixit, B. Barbeau, S. G. Mostafavi and M. Mohseni, *Sci. Total Environ.*, 2021, **754**, 142107.

249 T. T. Nguyen, X. Min, W. Xia, Z. Qiang, R. S. Khandge, H. K. Yu, J. W. Wang, Y. Wang and X. Ma, *J. Membr. Sci.*, 2024, **705**, 122925.

250 I. M. Manning, N. Guan, P. Chew, H. P. Macdonald, K. E. Miller, M. J. Strynar, O. Coronell and F. A. Leibfarth, *Angew. Chem.*, 2022, **134**, e202208150.

251 S. Deng, Q. Yu, J. Huang and G. Yu, *Water Res.*, 2010, **44**(18), 5188–5195.

252 Z. Du, S. Deng, Y. Chen, B. Wang, J. Huang, Y. Wang and G. Yu, *J. Hazard. Mater.*, 2015, **286**, 136–143.

253 Y. Gao, S. Deng, Z. Du, K. Liu and G. Yu, *J. Hazard. Mater.*, 2017, **323**, 550–557.

254 K. E. Carter and J. Farrell, *Sep. Sci. Technol.*, 2010, **45**(6), 762–767.

255 S. T. M. L. D. Senevirathna, S. Tanaka, S. Fujii, C. Kunacheva, H. Harada, B. R. Shivakoti and R. Okamoto, *Chemosphere*, 2010, **80**(6), 647–651.

256 E. Gagliano, M. Sgroi, P. P. Falciglia, F. G. A. Vagliasindi and P. Roccaro, *Water Res.*, 2020, **171**, 115381.

257 P. McCleaf, S. Englund, A. Östlund, K. Lindegren, K. Wiberg and L. Ahrens, *Water Res.*, 2017, **120**, 77–87.

258 A. Zaggia, L. Conte, L. Falletti, M. Fant and A. Chiorboli, *Water Res.*, 2016, **91**, 137–146.

259 L. Contea, L. Fallettia, A. Zaggiaa and M. Milanb, *Chem. Eng. Trans.*, 2015, **43**, 2257–2262.

260 F. Dixit, B. Barbeau, S. G. Mostafavi and M. Mohseni, *Water Res.*, 2020, **183**, 116098.

261 S. Woodard, J. Berry and B. Newman, *Remed. J.*, 2017, **27**, 19–27.

262 S. Che, B. Jin, Z. Liu, Y. Yu, J. Liu and Y. Men, *Environ. Sci. Technol. Lett.*, 2021, **8**, 668–674.

263 Y. Yu, S. Che, C. Ren, B. Jin, Z. Tian, J. Liu and Y. Men, *Environ. Sci. Technol.*, 2022, **56**, 4894–4904.

264 S. H. Yang, Y. Shi, M. Strynar and K. H. Chu, *J. Hazard. Mater.*, 2022, **423**, 127052.

265 L. P. Wackett and S. L. Robinson, *Biochem. J.*, 2020, **477**(15), 2875–2891.

266 M. Lewis, M. H. Kim, N. Wang and K. H. Chu, *Sci. Total Environ.*, 2016, **572**, 935–942.

267 D. M. J. Shaw, G. Munoz, E. M. Bottos, S. V. Duy, S. Sauvé, J. Liu and J. D. Van Hamme, *Sci. Total Environ.*, 2019, **647**, 690–698.

268 L. B. Yi, L. Y. Chai, Y. Xie, Q. J. Peng and Q. Z. Peng, *Genet. Mol. Res.*, 2016, **15**(2), 15028043.

269 B. G. Kwon, *Chemosphere*, 2015, **138**, 1039–1044.

270 S. P. Chetverikov, D. A. Sharipov, T. Y. Korshunova and O. N. Loginov, *Appl. Biochem. Microbiol.*, 2017, **53**, 533–538.

271 S. Huang and P. R. Jaffé, *Environ. Sci. Technol.*, 2019, **53**(19), 11410–11419.

272 S. P. Chetverikov, D. A. Sharipov, T. Y. Korshunova and O. N. Loginov, *Appl. Biochem. Microbiol.*, 2017, **53**(5), 533–538.

273 B. G. Kwon, H. J. Lim, S. H. Na, B. I. Choi, D. S. Shin and S. Y. Chung, *Chemosphere*, 2014, **109**, 221–225.

274 V. P. Beškoski, A. Yamamoto, T. Nakano, K. Yamamoto, C. Matsumura, M. Motegi, L. S. Beškoski and H. Inui, *Sci. Total Environ.*, 2018, **636**, 355–359.

275 B. D. Turner, S. W. Sloan and G. R. Currell, *Chemosphere*, 2019, **229**, 22–31.

276 D. M. J. Shaw, G. Munoz, E. M. Bottos, S. V. Duy, S. Sauvé, J. Liu and J. D. Van Hamme, *Sci. Total Environ.*, 2019, **647**, 690–698.

277 S. H. Yang, Y. Shi, M. Strynar and K. H. Chu, *J. Hazard. Mater.*, 2022, **423**, 127052.

278 M. Ruiz-Urigüen, W. Shuai, S. Huang and P. R. Jaffé, *Chemosphere*, 2022, **292**, 133506.

279 N. Wang, R. C. Buck, B. Szostek, L. M. Sulecki and B. W. Wolstenholme, *Chemosphere*, 2012, **87**, 527–534.

280 M. H. Kim, N. Wang and K. H. Chu, *Appl. Microbiol. Biotechnol.*, 2014, **98**, 1831–1840.

281 Y. Yu, K. Zhang, Z. Li, C. Ren, J. Chen, Y. H. Lin, J. Liu and Y. Men, *Environ. Sci. Technol.*, 2020, **54**, 14393–14402.

282 M. J. A. Dinglasan, Y. Ye, E. A. Edwards and S. A. Mabury, *Environ. Sci. Technol.*, 2004, **38**, 2857–2864.

283 C. Liu and J. Liu, *Environ. Pollut.*, 2016, **212**, 230–237.

284 H. Lee, J. Deon and S. A. Mabury, *Environ. Sci. Technol.*, 2010, **44**, 3305–3310.

285 J. Akhtar and N. A. S. Amin, *Renewable Sustainable Energy Rev.*, 2011, **15**(3), 1615–1624.

286 Y. Cao and A. Pawłowski, *Renewable Sustainable Energy Rev.*, 2012, **16**(3), 1657–1665.

287 B. Wu, S. Hao, Y. Choi, C. P. Higgins, R. Deeb and T. J. Strathmann, *Environ. Sci. Technol. Lett.*, 2019, **6**, 630–636.

288 H. Hori, Y. Nagaoka, A. Yamamoto, T. Sano, N. Yamashita, S. Taniyasu, S. Kutsuna, I. Osaka and R. Arakawa, *Environ. Sci. Technol.*, 2006, **40**, 1049–1054.

289 M. Pham, L. Schideman, B. K. Sharma, Y. Zhang and W. T. Chen, *Bioresour. Technol.*, 2013, **149**, 126–135.

290 M. Greger and T. Landberg, *J. Environ. Manage.*, 2024, **351**, 119895.

291 P. H. N. Vo, T. T. P. Nguyen, H. T. M. Nguyen, J. Baulch, S. Dong, C. V. Nguyen, P. K. Thai and A. V. Nguyen, *Water Res.*, 2024, **253**, 121300.

292 F. Rokhsar Talabazar, C. Baresel, R. 1 Ghorbani, I. Tzanakis, A. Koşar, D. Grishenkov and M. Ghorbani, *Chem. Eng. J.*, 2024, **495**, 153573.

293 E. Pensini, A. Dinardo, K. Lamont, J. Longstaffe, A. Elsayed and A. Singh, *Can. J. Civ. Eng.*, 2019, **46**, 881–886.

294 C. Zeng, S. Tanaka, Y. Suzuki and S. Fujii, *Chemosphere*, 2017, **183**, 599–604.

295 L. Li, T. Xiang, B. Su, H. Li, B. Qian and C. Zhao, *J. Appl. Polym. Sci.*, 2012, **123**, 2320–2329.

296 B. Niu, M. Yu, C. Sun, L. Wang, Y. Niu, H. Huang and Y. Zheng, *J. Nat. Fibers*, 2022, **19**, 2119–2128.

297 S. S. Elanchezhiyan, J. Preethi, K. Rathinam, L. K. Njaramba and C. M. Park, *Carbohydr. Polym.*, 2021, **267**, 118165.

298 C. Wu, M. J. Klemes, B. Trang, W. R. Dichtel and D. E. Helbling, *Water Res.*, 2020, **182**, 115950.

299 W. Cai, D. A. Navarro, J. Du, G. Ying, B. Yang, M. J. McLaughlin and R. S. Kookana, *Sci. Total Environ.*, 2022, **817**, 152975.

300 F. Wang, K. Shih, R. Ma and X. yan Li, *Chemosphere*, 2015, **131**, 178–183.

301 C. Y. Tang, Q. Shiang Fu, D. Gao, C. S. Criddle and J. O. Leckie, *Water Res.*, 2010, **44**, 2654–2662.

302 Z. Wang, I. T. Cousins, M. Scheringer and K. Hungerbuehler, *Environ. Int.*, 2015, **75**, 172–179.

303 T. Jina, M. Peydayesha and R. Mezzenga, *Environ. Int.*, 2021, **157**, 106876.

304 C. Eschauzier, E. Beerendonk, P. Scholte-Veenendaal and P. De Voogt, *Environ. Sci. Technol.*, 2012, **46**, 1708–1715.

305 Y. Yao, H. Zhu, H. Li, H. Hu, T. Zhang, E. Yamazaki, S. Taniyasu, N. Yamashita and H. Sun, *Ecotoxicol. Environ. Saf.*, 2014, **108**, 318–328.

306 J. Wang, L. Wang, C. Xu, R. Zhi, R. Miao, T. Liang, X. Yue, Y. Lv and T. Liu, *Chem. Eng. J.*, 2018, **332**, 787–797.

307 J. Eke, L. Banks, M. A. Mottaleb, A. J. Morris, O. V Tsyusko and I. C. Escobar, *Membranes*, 2021, **11**, 1–18.

308 S. Kurwadkar, J. Dane, S. R. Kanel, M. N. Nadagouda, R. W. Cawdrey, B. Ambade, G. C. Struckhoff and R. Wilkin, *Sci. Total Environ.*, 2022, **809**, 151003.

309 Q. Wang, Y. Ruan, H. Lin and P. K. Lam, *Sci. Total Environ.*, 2020, **737**, 139804.

310 J. Hammer and S. Endo, *Environ. Sci. Technol.*, 2022, **2022**, 15737–15745.

311 M. Ongwandee, T. Chatsuvan, W. Suksawas Na Ayudhya and J. Morris, *Environ. Sci. Pollut. Res.*, 2017, **24**, 5654–5668.

312 K. U. Goss, *Crit. Rev. Environ. Sci. Technol.*, 2004, **34**(4), 339–389.

313 J. N. Meegoda, J. A. Kewalramani, B. Li and R. W. Marsh, *Int. J. Environ. Res. Public Health*, 2020, **17**(21), 8117.

314 M. Shoeib, T. Harner and P. Vlahos, *Environ. Sci. Technol.*, 2006, **40**, 7577–7583.

315 R. Hunter Anderson, D. T. Adamson and H. F. Stroo, *J. Contam. Hydrol.*, 2019, **220**, 59–65.

316 A. K. Weber, L. B. Barber, D. R. Leblanc, E. M. Sunderland and C. D. Vecitis, *Environ. Sci. Technol.*, 2017, **51**, 4269–4279.

317 M. L. Brusseau, N. Yan, S. Van Glubt, Y. Wang, W. Chen, Y. Lyu, B. Dungan, K. C. Carroll and F. O. Holguin, *Water Res.*, 2019, **148**, 41–50.